Accurate Coupled Cluster Calculation of Nonlinear Optical Properties of Molecules

Christof Hättig

Institute of Nanotechnology
Forschungszentrum Karlsruhe,
P.O. Box 3640
D-76021 Karlsruhe

ABSTRACT

Recent developments in coupled cluster nonlinear response theory opened for the first time a route to accurate and systematic *ab initio* calculations of nonlinear optical and magneto-optical properties. The inclusion of the frequency-dependence (dispersion) at an electron correlated level and the use of systematic correlation consistent basis sets made it possible to achieve accuracies close to those of the best available experiments. The approach has in the mean time been applied to a number of nonlinear properties including frequency-dependent first and second hyperpolarizabilities, fifth harmonic generation, electric-field-gradient-induced birefringence, two-photon absorption, magnetic circular dichroism, Verdet constants, Cotton-Mouton constants, Kerr and ESHG second virial coefficients, etc.

Due to the quartic order of the coupled cluster equations, coupled cluster response theory can be cast into a lego-brick like structure with only a limited number of basic building blocks. This allowed to implement high-order response functions which have not been accessible before on an electron correlated level. We give a short review of the latest developments of coupled cluster nonlinear response theory and present a selected number of applications covering electric-field-induced second-harmonic generation, dc Kerr effect, degenerate four wave mixing, third-harmonic and fifth-harmonic generation and electric-field-gradient-induced birefringence to illustrate the strength of the approach.

1 INTRODUCTION

Response function approaches were introduced into the quantum chemistry literature about forty years ago [1–4]. At that time they were referred to as Green functions or propagator approaches. Soon after the introduction it became apparent that they offered a viable and attractive alternative to state specific approaches for obtaining molecular properties as excitation energies, transition moments and second-order molecular properties. In particular it was the only approach to efficient *ab initio* calculations on *frequency-dependent* properties.

The response function approaches have since developed into a useful tool, not only for calculating molecular properties related to the linear response but also for calculations of nonlinear optical and magneto-optical molecular properties. For most of the common electronic structure wave function models as f.x. Hartree-Fock self-consistent field (SCF), multiconfiguration self-consistent field (MCSCF), density functional theory (DFT), and a whole hierarchy of coupled cluster models (CCS, CC2, CCSD and CC3) linear and nonlinear response functions have been developed and have served as a useful tool for the calibration and interpretation of molecular properties. To give a specific example consider the history of the electric-field-induced second harmonic generation (ESHG) experiments of the second hyperpolarizability of Neon. Based on a sequence of ESHG measurements using lasers of different frequencies Shelton found that the dispersion of the ESHG hyperpolarizability of Ne was anomalous [5, 6], in contrast to the posi-

tive dispersion found in a previous experiment [7,8] and in an early multiconfiguration self-consistent field (MCSCF) calculation [9]. Based on an empirical calculation Bishop demonstrated [10] that the anomalous dispersion obtained in the ESHG experiment [5,6] can not be reproduced by theory. Large-scale MCSCF response function calculations were then carried out and showed that the dispersion was not anomalous [11]. Subsequently this was confirmed by new experimental ESHG data [12]. Recently accurate coupled cluster singles and doubles (CCSD) response function calculations have been carried out and have challenged the accuracy of one of the new ESHG data points [13]. This yet has to be confirmed by experiment. The above example demonstrates clearly the enormous development that has taken place since response functions were introduced. It also shows how important it is that the development in theory and experiment goes hand in hand and a number of reference molecules is established for which the nonlinear properties are known very accurately, so that they can serve as benchmark for assessing the accuracy of more approximate methods and as reference substances (external standards) in relative measurements.

For frequency-dependent hyperpolarizabilities an error tolerance of a couple of percents is still a difficult task that has been accomplished only for a few molecules. Such an accuracy requires a thorough treatment of dynamic electron correlation and large one-particle basis sets. To obtain an accurate description of the dispersion, the frequency-dependence must be accounted for at a correlated level using a wavefunction model where also the pole structure — i.e. the excitation energies — is described at a correlated level. This is in general only achieved by iterative correlation methods like multiconfiguration self-consistent field (MCSCF), configuration interaction (CI), or coupled cluster (CC) response theory. Until today, only the last method is capable of providing accurate results also for larger systems.

For molecules it is also necessary to consider the zero point vibrational averaging and the pure vibrational contributions to obtain a realistic comparison with experiment. The later contributions are particular difficult to evaluate since they require not only a model for the vibrational wavefunction, but also the polarizabilities and hyperpolarizabilities as functions of the internuclear distances or at least their geometric derivatives. In several cases it is these contributions which hamper today a more accurate *ab initio* calculation of the hyperpolarizabilities.

2 COUPLED CLUSTER NONLINEAR RESPONSE THEORY

In the derivation of response functions one considers a molecule or an atom described by the time-independent Hamiltonian $\hat{H}^{(0)}$ which is perturbed by an external one-electron perturbation $\hat{V}(t,\epsilon)$.

$$\hat{H}(t,\epsilon) \;=\; \hat{H}^{(0)} + \hat{V}(t,\epsilon) \tag{1}$$

We assume that the perturbation operator $\hat{V}(t,\epsilon)$ can be expanded in a sum over Fourier components as

$$\hat{V}(t,\epsilon) \;=\; \sum_j \hat{X}_j \epsilon_j e^{(-i\omega_j t)} \;\;, \tag{2}$$

where $\hat{X}_j$ are hermitian time- and field-independent one-electron operators and ϵ_j are associated field strengths. The letter ϵ without index is in the following used as abbreviation for the complete set $\{\epsilon_j\}$ of all field strengths included in $\hat{V}$. The time-dependent ground-state coupled cluster wavefunction for such a system is conveniently parameterized in a form, where the oscillating phase factor caused by the so-called level-shift or time-dependent quasienergy $\mathcal{W}(t,\epsilon)$ is explicitly isolated [14–17]:

$$\begin{aligned} |\mathrm{CC}(t,\epsilon)\rangle \;&=\; \exp\left(-i\int_{t_0}^{t}\mathcal{W}(t',\epsilon)dt'\right) \\ &\quad\times\exp\left(\hat{T}(t,\epsilon)\right)|\mathrm{HF}\rangle \end{aligned} \tag{3}$$

The field- and time-dependent cluster operator is defined as $\hat{T}(t,\epsilon) = \sum_\mu t_\mu(t,\epsilon)\hat{\tau}_\mu$ and $|\mathrm{HF}\rangle$ is the SCF wavefunction of the unperturbed molecule. By keeping the Hartree-Fock reference fixed in the presence of the external perturbation, a two step approach, which would introduce into the coupled cluster wavefunction an artificial pole structure from the response of the Hartree Fock orbitals, is avoided. The quasienergy $\mathcal{W}$ and the time-dependent coupled cluster equations are determined by projecting the time-dependent Schrödinger equation onto the Hartree-Fock reference and onto the bra states $\langle\mathrm{HF}|\hat{\tau}_\mu^\dagger\exp(-\hat{T})$:

$$\mathcal{W}(\epsilon,t) = \langle\mathrm{HF}|\hat{H}(\epsilon,t)\exp(\hat{T})|\mathrm{HF}\rangle. \tag{4}$$

$$\langle\mathrm{HF}|\hat{\tau}_\mu^\dagger\exp(-\hat{T})\hat{H}(t,\epsilon)\exp(\hat{T})|\mathrm{HF}\rangle - i\frac{d}{dt}t_\mu = 0 \tag{5}$$

The latter equation may be written in the shorthand form

$$e_\mu(t,\epsilon) - i\tfrac{d}{dt}t_\mu(t,\epsilon) \;=\; 0 \quad . \tag{6}$$

Frequency-dependent higher-order properties can now by obtained as derivatives of the time-average of the

quasienergy $\{\mathcal{W}\}_T$ with respect to the field strengths of the external perturbations. To derive computational efficient expressions for the derivatives of the coupled cluster quasienergy we use a variational formulation which is obtained by combining the quasienergy and the time-dependent coupled cluster equations to a quasienergy Lagrangian:

$$L(t,\epsilon) \;=\; \mathcal{W}(t,\epsilon) + \sum_{\mu} \bar{t}_{\mu} \Big(e_{\mu}(t,\epsilon) - i\tfrac{d}{dt} t_{\mu}) \Big) \qquad (7)$$

The time-average of the quasienergy Lagrangian

$$\{L(t,\epsilon)\}_T \;=\; \lim_{t_0\rightarrow\infty} \frac{1}{2t_0} \int_{-t_0}^{+t_0} L(t,\epsilon) dt \;\; , \qquad (8)$$

may now be required to be stationary with respect to the Fourier components of the cluster amplitudes and the Lagrangian multipliers [14, 17–19].

$$\delta\{L(t,\epsilon)\}_T \;=\; 0 \qquad (9)$$

The last equation thus constitutes a variation principle for the coupled cluster (quasi-)energy and the coupled cluster wavefunction within oscillating harmonic external fields.

The ansatz outlined above, combines the response function approach with usual derivative theory, as known for static (higher-order) properties. In the limit of static fields, all equations smoothly reduce to the usual equations for (unrelaxed) coupled cluster derivatives, which is an invaluable advantage for the implementation of the approach in quantum chemistry program packages.

If one now inserts a perturbation and Fourier expansion of the cluster amplitudes and the Lagrangian multipliers,

$$\begin{aligned} t_{\mu}(t,\epsilon) \;&=\; t_{\mu}^{(0)} + \sum_{n=1}^{\infty} \frac{1}{n!} \qquad (10) \\ &\times \sum_{j_1} \cdots \sum_{j_n} t^{X_{j_1}\ldots X_{j_n}}(\omega_{j_1},\ldots,\omega_{j_n}) \\ &\times \prod_{m=1}^{n} \epsilon_{j_m}(\omega_{j_m}) e^{-i\omega_{j_m} t} \end{aligned}$$

$$\begin{aligned} \bar{t}_{\mu}(t,\epsilon) \;&=\; \bar{t}_{\mu}^{(0)} + \sum_{n=1}^{\infty} \frac{1}{n!} \qquad (11) \\ &\times \sum_{j_1} \cdots \sum_{j_n} \bar{t}^{X_{j_1}\ldots X_{j_n}}(\omega_{j_1},\ldots,\omega_{j_n}) \\ &\times \prod_{m=1}^{n} \epsilon_{j_m}(\omega_{j_m}) e^{-i\omega_{j_m} t} \end{aligned}$$

the variational condition for the time-average of the quasienergy (9) becomes a set of linear equations for the individual expansion coefficients of $t_{\mu}(t,\epsilon)$ and $\bar{t}_{\mu}(t,\epsilon)$. In zeroth-order one obtains the usual coupled cluster equations, $e^{(0)} = 0$, and the equations for the zeroth-order Lagrangian multipliers,

$$\eta^{(0)} + \bar{t}^{(0)} \mathbf{A} \;=\; 0 \;\; , \qquad (12)$$

where the vector $\eta^{(0)}$ and the Jacobian matrix $\mathbf{A}$ are defined as partial derivatives of the quasienergy and the Lagrangian with respect to cluster amplitudes and Lagrangian multipliers:

$$\eta_{\nu}^{(0)} \;=\; \left(\frac{\partial \mathcal{W}}{\partial t_{\nu}} \right)_0 \;\; , \qquad (13)$$

$$A_{\mu\nu} \;=\; \left(\frac{\partial^2 L}{\partial \bar{t}_{\mu} \partial t_{\nu}} \right)_0 \;\; . \qquad (14)$$

The index 0 indicates that the derivatives are taken for zero perturbation strengths. The equations for the first-order amplitudes and multipliers are obtained as:

$$\Big(\mathbf{A} - \omega \mathbf{1} \Big) t^X(\omega) \;=\; -\xi^X \;\; , \qquad (15)$$

$$\bar{t}^X(\omega) \Big(\mathbf{A} + \omega \mathbf{1} \Big) \;=\; -\Big(\eta^X + \mathbf{F} t^X(\omega) \Big) \;\; , \qquad (16)$$

with ξ^X, η^X, and $\mathbf{F}$ defined as:

$$\xi_{\mu}^X \;=\; \left(\frac{\partial^2 L}{\partial \epsilon_X \partial \bar{t}_{\mu}} \right)_0 \;\; , \qquad (17)$$

$$\eta_{\mu}^X \;=\; \left(\frac{\partial^2 L}{\partial \epsilon_X \partial t_{\mu}} \right)_0 \;\; , \qquad (18)$$

$$F_{\mu\nu} \;=\; \left(\frac{\partial^2 L}{\partial t_{\mu} \partial t_{\nu}} \right)_0 \;\; . \qquad (19)$$

The second-order response equations for the cluster amplitudes and the Lagrangian multipliers are:

$$\Big(\mathbf{A} - (\omega_A + \omega_B) \mathbf{1} \Big) t^{AB}(\omega_A,\omega_B) = -\xi^{AB}(\omega_A,\omega_B), \qquad (20)$$

$$\bar{t}^{AB}(\omega_A,\omega_B) \Big(\mathbf{A} + (\omega_A + \omega_B) \mathbf{1} \Big) = -\bar{\xi}^{AB}(\omega_A,\omega_B), \qquad (21)$$

with the right-hand-side vectors defined as:

$$\begin{aligned} \xi^{AB}(\omega_A,\omega_B) \;&=\; \hat{P}^{AB} \big(\tfrac{1}{2} \mathbf{B} t^A(\omega_A) t^B(\omega_B) \qquad (22) \\ &\quad + \mathbf{A}^B t^A(\omega_A) \big) \;\; , \end{aligned}$$

$$\begin{aligned} \bar{\xi}^{AB}(\omega_A,\omega_B) \;&=\; \mathbf{F} t^{AB}(\omega_A,\omega_B) + \qquad (23) \\ &\quad \hat{P}^{AB} \big(\tfrac{1}{2} \mathbf{G} t^A(\omega_A) t^B(\omega_B) + \mathbf{F}^A t^B(\omega_B) \\ &\quad + \bar{T}^B(\omega_B) \mathbf{B} t^A(\omega_A) + \bar{T}^B(\omega_B) \mathbf{A}^A \big) \;\; . \end{aligned}$$

The matrices $\mathbf{B}$, $\mathbf{G}$ and $\mathbf{F}^X$ are defined as partial third derivatives of the Lagrangian:

$$G_{\mu\nu\gamma} = \left(\frac{\partial^3 L}{\partial t_\mu \partial t_\nu \partial t_\gamma}\right)_0 , \quad (24)$$

$$B_{\gamma\mu\nu} = \left(\frac{\partial^3 L}{\partial \bar{t}_\gamma \partial t_\mu \partial t_\nu}\right)_0 , \quad (25)$$

$$F^X_{\mu\nu} = \left(\frac{\partial^3 L}{\partial t_\mu \partial t_\nu \partial \epsilon_X}\right)_0 , \quad (26)$$

$$A^X_{\mu\nu} = \left(\frac{\partial^3 L}{\partial \bar{t}_\mu \partial t_\nu \partial \epsilon_X}\right)_0 . \quad (27)$$

To go beyond quadratic response theory, i.e. third-order properties, one needs in addition to the second partial derivatives of the Lagrangian defined in Eqs. (14) and (17) – (19) and the third partial derivatives defined in Eqs. (24) – (27) the fourth partial derivatives

$$H_{\mu\nu\gamma\delta} = \left(\frac{\partial^4 L}{\partial t_\mu \partial t_\nu \partial t_\gamma \partial t_\delta}\right)_0 , \quad (28)$$

$$C_{\mu\nu\gamma\delta} = \left(\frac{\partial^4 L}{\partial \bar{t}_\mu \partial t_\nu \partial t_\gamma \partial t_\delta}\right)_0 , \quad (29)$$

$$B^X_{\mu\nu\gamma} = \left(\frac{\partial^4 L}{\partial \bar{t}_\mu \partial t_\nu \partial t_\gamma \partial \epsilon_X}\right)_0 , \quad (30)$$

and the fifth partial derivative

$$D_{\mu\nu\gamma\delta\epsilon} = \left(\frac{\partial^5 L}{\partial \bar{t}_\mu \partial t_\nu \partial t_\gamma \partial t_\delta \partial t_\epsilon}\right)_0 . \quad (31)$$

Because the cluster equations are at most of quartic order in the cluster amplitudes, no higher partial derivatives of the Lagrangian exists. These *response matrices* form thus the basic building blocks of nonlinear coupled cluster response theory through any order. Once these "lego bricks" are implemented as program modules, setting up the right-hand-side vectors of the linear equations or the calculation of the contributions to the nonlinear properties is only a matter of putting these lego bricks together, i.e. calling the respective program modules with the right combination of amplitude vectors.

The response functions are obtained as derivatives of the real part of the time-averaged quasienergy Lagrangian:

$$\langle\langle X_1; X_2 \ldots, X_n\rangle\rangle_{\omega_2,\ldots,\omega_n} = \left(\frac{d^n \left\{\frac{1}{2}L(t,\epsilon) + \frac{1}{2}L(t,\epsilon)^*\right\}_T}{d\epsilon_1(\omega_1)\ldots d\epsilon_n(\omega_n)}\right)_0 \quad (32)$$

As a consequence of the time-averaging of the quasienergy Lagrangian, the derivative in the last equation gives only a nonvanishing result if the frequencies of the external fields fulfill the matching condition $\sum_i \omega_i = 0$. For example, in fourth order Eq. (32) gives the cubic response function:

$$\begin{aligned}\langle\langle A; B, C, D\rangle\rangle_{\omega_B,\omega_C,\omega_D} = \quad (33)\\ \frac{1}{2}\hat{C}^{\pm\omega}\hat{P}^{ABCD}\Big\{\tfrac{1}{24}\mathbf{H}t^A(\omega_A)t^B(\omega_B)t^C(\omega_C)t^D(\omega_D)\\ +\tfrac{1}{4}\Big(\eta^{CD}(\omega_C,\omega_D) + \frac{1}{2}\mathbf{F}t^{CD}(\omega_C,\omega_D)\Big)t^{AB}(\omega_A,\omega_B)\\ +\tfrac{1}{6}\bar{t}^A(\omega_A)\mathbf{C}t^B(\omega_B)t^C(\omega_C)t^D(\omega_D)\\ +\frac{1}{2}\bar{t}^A(\omega_A)\ \mathbf{B}^B\ t^C(\omega_C)\ t^D(\omega_D)\Big\},\end{aligned}$$

with $\omega_A = -(\omega_B + \omega_C + \omega_D)$ and the vector η^{CD} defined as

$$\eta^{CD}(\omega_C,\omega_D) = \bar{\xi}^{CD}(\omega_C,\omega_D) - \mathbf{F}t^{CD}(\omega_C,\omega_D) . \quad (34)$$

The operator $\hat{P}^{ABCD}$ symmetrizes with respect to permutations of the perturbation indices A, B, C and D and the accompanied frequencies and $\hat{C}^{\pm\omega}$ symmetrizes with respect to an inversion of the signs of all frequencies and simultaneous complex conjugation.

Open-ended expressions for the coupled cluster nonlinear response functions and for the right-hand-side vectors of the response equations have been reported in the appendix of Ref. [20]. The approach outlined above was used between 1996 and 1998 to implement the response functions for the coupled cluster models CCS, CC2 and CCSD through pentic order, i.e. sixth-order properties [18, 19, 21–29] and are today available as part of the DALTON program package [30]. An implementation of the quadratic response function for the CC3 model, which accounts for connected triple excitations, was reported 1998 by Gauss and *et al.* [31].

3 FREQUENCY-DEPENDENT FIRST HYPERPOLARIZABILITY OF FH

A since almost two decades ongoing problem is the second harmonic generation first hyperpolarizability $\beta^{SHG}_{||}$ of the FH molecule. For second harmonic generation the experimental data must be compared with the hyperpolarizability component

$$\beta_{||} = \sum_{i=x,y,z} \frac{1}{5}\Big(\beta_{iiz} + \beta_{izi} + \beta zii\Big) , \quad (35)$$

Table 1: Basis set dependence of the (static) first hyperpolarizability of FH at the (unrelaxed) CCSD level. $R_e = 1.7328$ au. The direction of the positive z axis is from F to H. All numbers in atomic units.

Basis Set	β_{zzz}	β_{zxx}	$\beta_{\|\|}$
aug-cc-pVDZ	-12.14	-1.70	-9.32
d-aug-cc-pVDZ	-8.63	-0.69	-6.01
t-aug-cc-pVDZ	-8.92	-0.78	-6.29
q-aug-cc-pVDZ	-9.03	-0.82	-6.40
aug-cc-pVTZ	-11.57	-2.38	-9.80
d-aug-cc-pVTZ	-9.76	-1.52	-7.68
t-aug-cc-pVTZ	-9.84	-1.69	-7.93
q-aug-cc-pVTZ	-9.80	-1.71	-7.93
aug-cc-pVQZ	-10.47	-1.96	-8.63
d-aug-cc-pVQZ	-9.75	-1.57	-7.73
t-aug-cc-pVQZ	-9.77	-1.67	-7.87
q-aug-cc-pVQZ	-9.79	-1.64	-7.84
aug-cc-pV5Z	-10.07	-1.87	-8.29
d-aug-cc-pV5Z	-9.77	-1.59	-7.77

Table 2: Convergence of the (static) first hyperpolarizability of FH with the correlation treatment. Results are taken from Ref. [34]; $R_e = 1.7328795$ au; aug-cc-pVDZ basis; all numbers in atomic units.

Method	β_{zzz}	β_{zxx}	$\beta_{\|\|}$
CCS	-11.652	-1.061	-8.264
CC2	-14.664	-2.475	-11.768
CCSD	-12.145	-1.706	-9.334
CC3	-11.673	-1.574	-8.893
CCSDT	-11.774		
FCI	-11.614	-1.548	-8.826
Error			
CCS	-0.037	0.487	0.562
CC2	-3.050	-0.931	-2.947
CCSD	-0.531	-0.159	-0.509
CC3	-0.058	-0.027	-0.067
CCSDT	-0.160		

where the z axis is that of the permanent dipole moment. For a linear molecule Eq. (35) reduces to

$$\beta_{||}^{SHG}(\omega) = \frac{1}{5}\Big(3\beta_{zzz}(-2\omega;\omega,\omega) + 2\beta_{zxx}(-2\omega;\omega,\omega) + 4\beta_{xzx}(-2\omega;\omega,\omega)\Big) , \quad (36)$$

Since its experimental determination by Dudley and Ward in 1985 [32] and the first *ab initio* calculations by Sekino and Bartlett [33] one year later, there has been a discussion in the literature whether the theoretical results are in agreement or in disagreement with the experiment. But still today both the experimental and the theoretical values are not known much better then $\approx \pm 5 - 10\%$. The experimental determination of $\beta_{||}^{SHG}$ is a non-trivial task since $\beta_{||}^{SHG}$ can not be determined directly, but must be extrapolated from the temperature-dependence of the (total) second harmonic generation hyperpolarizability, which itself is already difficult to measure accurately. However, accurate *ab initio* calculations for $\beta_{||}^{SHG}$ encounter also a number of difficulties: since β as a third-rank tensor is a purely anisotropic property the combination of components needed for $\beta_{||}^{SHG}$ is very sensitive to a balanced treatment of the three directions x, y, and z and the ground and the excited states [34]. This requires large accurate basis sets and a high-order correlation treatment which includes connected triple excitations. In Table 1 the static CCSD results for first hyperpolarizability components of FH are listed for the correlation consistent basis sets [35–39] x-aug-cc-pVXZ with X = D, T, Q, and 5 and x = d, t, q. The results demonstrate that convergence of $\beta_{||}$ within 1 au or $\pm 10\%$ requires at least a triple-ζ basis set and at least double augmentation. Convergence within $\pm 1\%$ for $\beta_{||}$ is not obtained before the d-aug-cc-pV5Z basis, which already consists of 207 functions. But even more severe than the basis set issue is the slow convergence with respect to the correlation treatment. The later can only be tested with FCI or other highly correlated methods in relatively small basis sets insufficient for really accurate results, but nevertheless are such benchmark calculations invaluable to obtain an impression how large the correlation error for a given method might be. For the first hyperpolarizability of FH, such calculations are available from Ref. [34]. The static results are listed in Table 2. It turns out that in particular for FH $\beta_{||}$ is extremely sensitive to the correlation treatment. At the CCSD level, which usually provide quite accurate results for polarizabilities and hyperpolarizabilities, $\beta_{||}$ for FH is still in error by ≈ -0.5 au or $\approx 6\%$ and even the CC3 model, which also accounts for connected triple excitations, is off by $\approx 0.75\%$. Thus to solve the electronic problem with an accuracy better than $\approx \pm 2\%$ requires in this case rather expensive calculations. But even if the electronic hyperpolarizability

Table 3: The second harmonic generation hyperpolarizability $\beta_{||}^{SHG}$ of FH at the ruby laser frequency of 694.3 nm. Results are in atomic units.

	$\beta_{||}^{SHG}(\omega)$
CC3 at $R_e = 1.7328$ au[a]	-8.32
+ zero point vibr. averag.[b]	-0.72
+ pure vib. contrib.[b]	-0.64
+ est. remain. basis effects[b]	$+0.16$
+ est. remain. correl. effects[b]	$+0.07$
best theoretical estimate[b]	-9.45 ± 0.5
experimental value[c]	-10.9 ± 1.0

[a] CC3 in the t-aug-cc-pVTZ basis, Ref. [31].
[b] see text. [c] Ref. [32].

$\beta_{||}^{SHG,e}$ is accurately known at the equilibrium distance, this is not the final answer. To compare directly with the experimental result for $\beta_{||}^{SHG}$ the electronic contribution $\beta_{||}^{SHG,e}$ must be averaged over the vibrational ground state wavefunction and the pure vibrational contribution $\beta_{||}^{SHG}$ must be added. Using a CCSD(T) potential energy curve and CCSD results for $\beta_{||}^{SHG}(\omega)$ as function of the internuclear distance, one obtains for the effect of vibrational averaging -0.72 au at $\lambda = 694.3$ nm. To evaluate the pure vibrational contribution, in addition to the potential energy curve also the dipole moment and polarizabilities at the frequencies ω and 2ω are needed as functions of the internuclear distance. Using again CCSD results for these properties, one finds for the pure vibrational contribution -0.64 au. Estimating the remaining basis set effects from the difference between the d-aug-cc-pV5Z and the t-aug-cc-pVTZ results from Table 1 and the remaining correlation effects from the difference between the FCI and the CC3 results from Table 2, one arrives at a best theoretical estimate for $\beta_{||}^{SHG}(694.3\mathrm{nm})$ of -9.45 ± 0.5 au, as shown in Table 3. The later estimate includes for the remaining higher-order correlation effects and the remaining basis set effects uncertainties of 0.1 au. The uncertainties for the effect of vibrational averaging and for the pure vibrational contributions are estimated as 0.1 au and 0.2 au, respectively.

The experimental value is with -10.9 ± 1.0 au somewhat larger. However, the uncertainties of the theoretical and the experimental value are too large to conclude from this a disagreement between theory and experiment. But anyway, an experimental reinvestigation of $\beta_{||}^{SHG}$ for FH would be quite helpful, in particular since the measurement of Ref. [32] was with respect to CF_4 as reference substance, for which the hyperpolarizability is also not known very accurately.

4 FREQUENCY-DEPENDENT SECOND HYPERPOLARIZABILITIES OF SMALL MOLECULES

Even though one might expect the opposite, the calculation of second hyperpolarizabilities turns in practice out to be easier than the calculation of the first hyperpolarizabilities, at least as long as it concerns the electronic contribution.

For the four optical processes we shall consider, the frequency arguments of the second hyperpolarizability are conventionally defined as [40]: $\gamma_{\mu\nu\eta\xi}^{dcKerr}(\omega) = \gamma_{\mu\nu\eta\xi}(-\omega;0,0,\omega)$, $\gamma_{\mu\nu\eta\xi}^{DFWM}(\omega) = \gamma_{\mu\nu\eta\xi}(-\omega;\omega,\omega,-\omega)$, $\gamma_{\mu\nu\eta\xi}^{ESHG}(\omega) = \gamma_{\mu\nu\eta\xi}(-2\omega;\omega,\omega,0)$, and $\gamma_{\mu\nu\eta\xi}^{THG}(\omega) = \gamma_{\mu\nu\eta\xi}(-3\omega;\omega,\omega,\omega)$. Note that for each of these hyperpolarizabilities the second and the third frequency argument are the same and that therefore the hyperpolarizabilities are symmetric in the second and third index, ν and η.

In most ESHG and THG experiments the measured tensor component is the isotropic average [40]:

$$\gamma_{||} \;=\; \frac{1}{15}\sum_{\xi\eta}\Big(\gamma_{\xi\xi\eta\eta} + \gamma_{\xi\eta\eta\xi} + \gamma_{\xi\eta\xi\eta}\Big)\;, \quad \xi,\eta = x,y,z\;. \tag{37}$$

Only few ESHG experiments exist for the 'perpendicular' isotropic tensor component [40,41]:

$$\gamma_{\perp} \;=\; \frac{1}{15}\sum_{\xi\eta}\Big(2\gamma_{\xi\eta\eta\xi} - \gamma_{\xi\xi\eta\eta}\Big)\;, \qquad \xi,\eta = x,y,z\;. \tag{38}$$

For the dc Kerr effect the tensor component relevant for comparison with experiment is [40]:

$$\gamma_K \;=\; \frac{3}{2}\big(\gamma_{||} - \gamma_{\perp}\big)\;. \tag{39}$$

For atoms $\gamma_{xxzz} + \gamma_{xzzx} + \gamma_{xzxz} = \gamma_{zzzz}$ and therefore $\gamma_{||} = \gamma_{zzzz}$ and $\gamma_{\perp} = \gamma_{zxxz}$ and the Kerr hyperpolarizability becomes $\gamma_K = 3/2(\gamma_{zzzz} - \gamma_{zxxz})$. For spherical top molecules (3 equivalent principal axes) $\gamma_{||}$ and $\gamma_{\perp}$ become:

$$\gamma_{||} \;=\; \tfrac{3}{5}\gamma_{zzzz} + \tfrac{2}{5}\gamma_{xxzz} + \tfrac{2}{5}\gamma_{zxxz} + \tfrac{2}{5}\gamma_{xzxz}\;, \tag{40}$$

$$\gamma_{\perp} \;=\; \tfrac{1}{5}\gamma_{zzzz} + \tfrac{4}{5}\gamma_{zxxz} - \tfrac{2}{5}\gamma_{xxzz}\;. \tag{41}$$

Using that for linear molecules $\gamma_{xxyy} + \gamma_{xyyx} + \gamma_{xyxy} = \gamma_{xxxx}$, the tensor components $\gamma_{||}$ and $\gamma_{\perp}$ can be reduced to:

$$\gamma_{||} = \frac{1}{15}\Big(8\gamma_{xxxx} + 2\gamma_{xxzz} + 2\gamma_{zzxx} + 2\gamma_{zxxz} + 2\gamma_{xzzx} + 2\gamma_{xzxz} + 2\gamma_{zxzx} + 3\gamma_{zzzz}\Big) \quad (42)$$

$$\gamma_{\perp} = \frac{1}{15}\Big(\gamma_{xxxx} + 5\gamma_{xyyx} + 4\gamma_{zxxz} - 2\gamma_{xxzz} + 4\gamma_{xzzx} - 2\gamma_{zzxx} + \gamma_{zzzz}\Big) \quad (43)$$

Independent of the spatial symmetry of the molecule or atom, the isotropic components $\gamma_{||}$, $\gamma_{\perp}$, and γ_K become in the static limit $\gamma_{||} = 3\gamma_{\perp} = \gamma_K = \gamma_0$.

In the single point calculations for the molecules N_2 and CH_4 equilibrium internuclear distances of r_{NN} = 2.074 au and r_{CH} = 2.052 au [42,43] were used [44] and for the sulphurhexafluoride molecule SF_6 a S—F bond distance of 1.564 Å was employed. In the CCS, CC2 and CCSD response calculations for Ne, Ar, CH_4 and SF_6 a frozen core approximation was used, if not stated otherwise. For the individual systems the following orbital occupations were kept frozen: Ne: $1s^2$, Ar: $1s^2 2s^2 2p^6$, CH_4: $1a_1^2$, SF_6: $1a_{1g}^2 2a_{1g}^2 1t_{1u}^6 1e_g^4 3a_{1g}^2 2t_{1u}^6$. No frozen core approximation was used for N_2 or in the SCF calculations. For the SCF hyperpolarizability calculations the cubic response function implementation [45] in the DALTON program package [46] was employed. In all calculations the correlation consistent basis sets developed by Dunning and coworkers [35–38,47] were used.

4.1 BASIS SET INVESTIGATION

Tables 4 and 5 list the results of a basis set study at the SCF and the (unrelaxed) CCSD level. For each fixed x-aug level the x-aug-cc-pVXZ series of correlation consistent basis sets converge to a valence basis set limit if the XZ level is increased successively. If for a fixed XZ level the augmentation x is increased the results converge to a series limit which is different from the basis set limit. In particular for the second hyperpolarizabilities of atoms and linear molecules it is well known that f functions are crucial already at the SCF level and thus accurate results can not be expected from the double-zeta basis sets x-aug-cc-pVDZ. For molecules with a two- or three-dimensional structure f functions are less important for γ_0, as is seen from the results for CH_4 and SF_6. As already found by Woon and Dunning in an earlier basis set study [38], polarizabilities and hyperpolarizabilities converge slowly in XZ if the augmentation level is low, which reflects the important role of diffuse functions for these properties. For Ne and Ar one obtains both at the Hartree-Fock and at the CCSD level an acceptable convergence in the triply-augmented series. The fourth set of diffuse functions improves slightly the convergence, but in the correlated calculations an increase of the cardinal number X becomes at the triply-augmented level more important than further augmentation with diffuse functions. For the diatomic molecule N_2 the convergence with the basis sets is somewhat faster than for the rare gas atoms. For N_2 already in the doubly-augmented series an increase of the cardinal number X is of the same importance as the inclusion of a third augmentation level. Also for methane and sulphurhexafluoride we find a considerable faster convergence than for atoms: For CH_4 at the SCF level the effects of going from the d-aug-cc-pVTZ basis to the next higher XZ or x-aug are small and the correlation contribution changes for CH_4 only little with the basis sets. This is somewhat different for SF_6 where the correlation contribution changes considerable both from the singly-augmented series to the doubly-augmented series and between the double-ζ and the triple-ζ basis sets.

At the Hartree-Fock level the hyperpolarizability usu-

Table 4: Static isotropic hyperpolarizabilities $\gamma_{||}(0)$ at the Hatree-Fock level as a function of basis set. The Ne, Ar, N_2 and CH_4 results are taken from Ref. [44].

	Ne	Ar	N_2	CH_4	SF_6
aug-cc-pVDZ	20.3	296	456	1497	737
aug-cc-pVTZ	28.3	456	560	1745	734
aug-cc-pVQZ	38.6	685	654	1830	782
aug-cc-pV5Z	50.1	741	685	....	....
d-aug-cc-pVDZ	49.3	718	672	1774	839
d-aug-cc-pVTZ	57.3	841	697	1868	837
d-aug-cc-pVQZ	62.0	890	710	1864	830
d-aug-cc-pV5Z	67.5	944	714	....	....
t-aug-cc-pVDZ	53.2	704	669	1815	....
t-aug-cc-pVTZ	66.5	941	710	1869	842
t-aug-cc-pVQZ	67.8	947	713	1868	....
t-aug-cc-pV5Z	68.6	961	....	....	....
q-aug-cc-pVDZ	53.3	706	680	1816	....
q-aug-cc-pVTZ	68.9	947	717	1871	....
q-aug-cc-pVQZ	68.5	953	715	....	....
q-aug-cc-pV5Z	68.7	961	....	....	....

Table 5: Static isotropic hyperpolarizabilities $\gamma_{||}(0)$ at the CCSD level as a function of basis set. The Ne, Ar, N_2 and CH_4 results are taken from Ref. [44].

	Ne	Ar	N_2	CH_4	SF_6
aug-cc-pVDZ	29.6	376	684	1931	1341
aug-cc-pVTZ	42.2	579	745	2199	1302
aug-cc-pVQZ	58.5	854	822	2285	....
aug-cc-pV5Z	76.8	914	844	....	....
d-aug-cc-pVDZ	83.9	990	938	2328	1581
d-aug-cc-pVTZ	94.2	1092	895	2364	1507
d-aug-cc-pVQZ	100.2	1110	881	2330	....
d-aug-cc-pV5Z	108.0	1159	873	....	....
t-aug-cc-pVDZ	94.4	975	935	2378	....
t-aug-cc-pVTZ	110.3	1218	903	2365	....
t-aug-cc-pVQZ	110.0	1179	883	....	....
t-aug-cc-pV5Z	110.2	1179	....	....	....
q-aug-cc-pVDZ	94.5	976	943	2380	....
q-aug-cc-pVTZ	114.5	1226	909	....	....
q-aug-cc-pVQZ	111.2	1186	....	....	....
q-aug-cc-pV5Z	110.2	1179	....	....	....

ally increases both, if x-aug or XZ is increased. For the correlation contribution to the hyperpolarizability the convergence pattern is dominated by different effects: In the CCSD response calculations an increase of γ_0 with the cardinal number X is only found for the lower augmentation levels. We find beyond singly-augmentation for N_2 and CH_4 and beyond doubly-augmentation for Ne and Ar a decrease of the hyperpolarizability if the correlation of the valence orbitals is improved in the series pVTZ – pVQZ – pV5Z. In particular for N_2 and CH_4, the correlation contribution to γ_0 is not much affected by the x-aug level. But for all three molecules N_2, CH_4 and SF_6 γ_0 decreases considerable if the correlation of the valence orbitals is improved by increasing the ζ-level of the basis set. Many correlated hyperpolarizability calculations in the literature were performed with basis sets of triple-zeta or similar quality and basis set convergence was often only explored with respect to augmentation with diffuse functions. From the above observation one may conclude that many of these studies obtained too large results for γ and underestimated the remaining basis set errors.

For neon and argon the SCF basis set limit is known from numerical Hartree-Fock calculations as $\gamma_0(\mathrm{Ne})$ = 69.3 au and $\gamma_0(\mathrm{Ar})$ = 966 au [48]. With the t-aug-cc-pV5Z basis sets, which were used in subsequent frequency-dependent calculations, the remaining basis set errors in the Hartree-Fock calculations are 0.7% (Ne) and 0.5% (Ar). At the CCSD level these basis sets give γ_0 = 110.2 au for Ne and γ_0 = 1178.5 au for Ar, when the core orbitals are frozen. With all electrons correlated the results in the same basis sets are $\gamma_0^{\mathrm{Ne}} = 109.3$ au and $\gamma_0^{\mathrm{Ar}} = 1172$ au. Because of the slower convergence of the correlated calculations the remaining basis set errors in the t-aug-cc-pV5Z basis should at the CCSD level be larger than in the Hartree-Fock calculations, probably in the range of 1 – 3%.

For N_2 and CH_4 the Hartree-Fock limit at the equilibrium geometries for γ_0 is estimated — based on the calculations in the largest basis sets — as 715±2 au and 1865±5 au, respectively. For the subsequent frequency-dependent calculations for both molecules the t-aug-cc-pVTZ basis set was used. At the CCSD level this basis gives γ_0 = 903.0 au for N_2 and γ_0 = 2364.8 au for CH_4, where for the latter molecule the $1a_1^2$ orbital occupation was kept frozen. In the corresponding core-valence sets, t-aug-cc-pCVTZ, one obtains with all electrons correlated $\gamma_0^{\mathrm{N_2}}$ = 896.3 au and $\gamma_0^{\mathrm{CH_4}}$ = 2353 au, corresponding to core effects of -6.7 au for N_2 and -12 au for CH_4. To obtain estimates for the remaining basis set errors at the correlated level, CCSD response calculations with larger basis set were carried out for the static hyperpolarizabilities. For the N_2 molecule the largest basis set used was the d-aug-cc-pV5Z basis, consisting of a $[8s7p6d5f4g3h]$ contraction with 326 basis functions. At the CCSD response level this basis set gives γ_0 = 873.2 au. Adding to this result the core correction of -6.7 au, one obtains a best estimate for the unrelaxed CCSD basis set limit of 867±7 au for the static second hyperpolarizability of N_2 at the equilibrium distance $r_e = 2.074$ au. For methane the largest basis set used was the d-aug-cc-pVQZ basis which consists of a $(14s8p5d4f3g)/[7s6p5d4f3g]$ contraction at the carbon atom and a $(8s5p4d3f)/[6s5p4d3f]$ contraction at the hydrogen atom, giving in total 353 basis functions. This basis set gives at the CCSD level for the static second hyperpolarizability of the methane molecule a result of 2329.6 au. Adding the estimate for the core effect obtained with the t-aug-cc-pVTZ and t-aug-cc-pCVTZ basis sets (-12 au), one obtains a best estimate for the unrelaxed CCSD basis set limit for the static second hyperpolarizability of CH_4 of 2318±35 au. For sulphurhexafluoride it is not possible to perform CCSD calculations for the second hyperpolarizability in a basis set which is close enough to convergence, to give a reliable esti-

Table 6: Static isotropic hyperpolarizabilities γ_0 obtained at different levels of the coupled cluster hierarchies and with and without the inclusion of core correlation effects.

	Ne	Ar	N_2	CH_4
CCS unrelaxed	78.2[a]	1154[a]	824.9[b]	2228[b]
CC2 unrelaxed	135.8[a]	1247[a]	991.9[b]	2557[b]
CCSD unrelaxed	110.2[a]	1178[a]	903.0[b]	2365[b]
			895.3[c]	2364[c]
SCF	68.6[a]	961[a]	710.1[b]	1869[b]
CCSD relaxed	99.1[a]	1106[a]	853.6[c]	2176[c]
CCSD rel. eff.[d]	−11.1[a]	−72[a]	−41.7[c]	−188[c]
CCSD(T) relax.	107.8[a]	1168[a]	910.7[c]	2294[c]
rel. & T_3 eff.[e]	−2.4[a]	−10[a]	15.4[c]	−70[c]

[a]t-aug-cc-pV5Z basis. [b]t-aug-cc-pVTZ basis. [c]d-aug-cc-pVTZ basis. [d]Difference between relaxed CCSD and unrelaxed CCSD results. [e]Difference between relaxed CCSD(T) and unrelaxed CCSD results.

Table 7: Third harmonic generation hyperpolarizabilities $\gamma_{||}(-3\omega;\omega,\omega,\omega)$ for Ne. Comparison of SCF, CCS, CC2 and CCSD dispersion curves for the q-aug-cc-pV5Z basis.

λ/nm	ω/au	SCF	CCS	CC2	CCSD
∞	.000000	68.64	78.20	135.8	110.2
2278.2	.020000	69.40	79.03	137.7	111.7
1319.0	.034544	70.95	80.71	141.7	114.6
1064.0	.042823	72.24	82.11	145.0	117.1
1055.0	.043188	72.30	82.18	145.1	117.2
911.3	.050000	73.62	83.61	148.6	119.7
694.3	.065625	77.57	87.90	159.0	127.4
632.8	.072003	79.61	90.11	164.5	131.5
590.0	.077226	81.49	92.15	169.6	135.2
514.5	.088558	86.31	97.37	183.0	144.9
488.0	.093368	88.71	99.96	189.8	149.8
457.9	.099505	92.12	103.65	199.7	156.9
455.6	.100000	92.42	103.97	200.5	157.5

mate for the CCSD basis set limit of γ_0. Even with the largest and best basis set — d-aug-cc-pVTZ — which consist for SF_6 of 438 contracted functions, it is not clear whether the result is converged better than within ± 80 au or $\pm 5\%$.

4.2 COMPARISON OF DIFFERENT WAVEFUNCTION MODELS

In the coupled cluster response approach the non-relaxed Hartree-Fock wavefunction of the unperturbed system is used as reference state in the coupled cluster calculation. In the static limit this becomes equivalent to finite field calculations where the external perturbation is first included in the Hamiltonian after the SCF step. Alternatively, in the orbital-relaxed coupled cluster approach the perturbation is already included in the SCF step. In orbital-relaxed CCS calculation the cluster amplitudes become zero and therefore the CCS ground state energy and properties become equal to the SCF results. For frequency-dependent properties the explicite treatment of orbital relaxation would lead to artificial poles in the correlated results for frequencies at which the SCF response functions become singular. However, in the static limit both, the non-relaxed coupled cluster response hierarchy CCS, CC2, CCSD, etc. and the orbital-relaxed SCF, CC2, CCSD, etc. are applicable and both hierarchies converge in the limit of a complete cluster expansion to the full CI treatment. The question arises, how efficient orbital relaxation can be treated implicitly by the single excitation manifold of the cluster operator. In the literature it is usually assumed that the orbital-relaxed hierarchy is more reliable. Numerical investigations [34, 49, 50] of this aspect, however, did not find a significant better performance of orbital-relaxed calculations compared to non-relaxed ones. In order to compare the performance of the two coupled cluster hierarchies for the hyperpolarizabilities the static limit values, γ_0, have been calculated for Ne, Ar, N_2 and CH_4, using the unrelaxed CCS, CC2 and CCSD response approaches and the orbital-relaxed SCF, CCSD and CCSD(T) models (see Table 6). The first elements in the two hierarchies, non-relaxed CCS and orbital-relaxed SCF, give for these examples results of similar accuracy, with the CCS values for all four systems between the SCF and the CCSD results; for Ne and N_2 closer to SCF and for Ar and CH_4 closer to CCSD. This indicates that orbital relaxation can efficiently be treated implicitly by the single excitation manifold of the cluster operator. From SCF to CCSD(T) the results for γ_0 increase by $\approx 60\%$ for Ne and by 20 – 30% for Ar, N_2, and CH_4, reflecting the well-known large effects of dynamic electron corre-

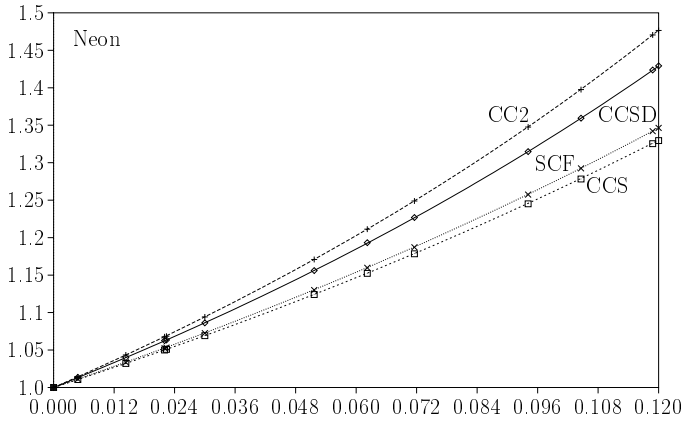


Figure 1: Comparison of the relative dispersion $\gamma_{||}(\omega)/\gamma_{||}(0)$ in the SCF, CCS, CC2 and CCSD response approaches for the third harmonic generation in the Neon atom. Ref. [44]

lation on the magnitude of γ_0. If one compares unrelaxed CC2 with the CCSD and CCSD(T) calculations, one finds that the CC2 response approach significantly overshoots the correlation contribution for all four examples. In the static limit CC2 is almost no improvement upon CCS. For all four examples the difference between unrelaxed CCSD and orbital-relaxed CCSD(T) values is only a small effect: Ne: 2.2%, Ar: 0.8%, N_2: 1.7% and CH_4: 3.1%. The difference between orbital-relaxed CCSD and CCSD(T) results is much larger: Ne: 8.8%, Ar: 5.6%, N_2: 6.7% and CH_4: 8.2%. If one assumes that the orbital-relaxed CCSD(T) values are close to the full CI limit, one thus finds that the remaining correlation error for the hyperpolarizabilities are larger in the orbital-relaxed CCSD calculations than in the unrelaxed CCSD response approach. From these results there is thus no reason to expect improvements by treating orbital relaxation explicitely in hyperpolarizability calculations with coupled cluster wavefunctions. To compare the description of the dispersion in SCF, CCS, CC2 and CCSD Table 7 gives some results for the third harmonic generation hyperpolarizability of the neon atom. In the literature is has been speculated that the dispersion contribution to the hyperpolarizabilities might be less sensitive to basis set selection and electron correlation treatment than the static hyperpolarizabilities [12, 40]. This suspection was based on a comparison of results obtained from SCF, MCSCF and MP2 calculations. However, the curvature of the dispersion curves is sensitive to the position of the first pole in $\gamma(\omega)$ and is thus sensitive to the lowest excitation energy. As the MP2 frequency-dependent properties have their lowest pole at the same position as

Table 8: Dispersion curves for different optical processes for $\gamma_{||}$ of Ne, calculated at the CCSD level using the t-aug-cc-pV5Z basis.

λ/nm	ω/au	Kerr[a]	DFWM	ESHG	THG
∞	.000000	110.2	110.2	110.2	110.2
2278.2	.020000	110.4	110.7	110.9	111.7
1319.0	.034544	110.9	111.6	112.4	114.6
1064.0	.042823	111.3	112.4	113.6	117.1
1055.0	.043188	111.3	112.5	113.6	117.2
911.3	.050000	111.7	113.3	114.8	119.7
694.3	.065625	112.8	115.5	118.3	127.4
632.8	.072003	113.4	116.7	120.1	131.5
590.0	.077226	113.9	117.7	121.7	135.2
514.5	.088558	115.0	120.2	125.7	144.9
488.0	.093368	115.6	121.4	127.7	149.8
457.9	.099505	116.4	123.1	130.4	156.9
455.6	.100000	116.4	123.2	130.6	157.5

[a]For the Kerr process the table list γ_K. For the definition of γ_K see Sec. 4.

in SCF [51, 52], it is not surprising that the MP2 dispersion is usually similar to the SCF dispersion. In Figure 1 the ratio $\gamma_{||}^{\mathrm{THG}}(\omega)/\gamma_0$ is plotted for the neon atom at the SCF, CCS, CC2 and CCSD level. From this plot it is obvious that dynamic correlation has as large effects on the dispersion of the hyperpolarizability as it has on the static hyperpolarizability. The dispersion of γ is strongly underestimated by the uncorrelated SCF and CCS methods, which give very similar results for the dispersion. Despite the disappointing performance of CC2 for the absolute magnitude of γ, the relative dispersion effect $\gamma^{THG}(\omega)/\gamma_0$ is at the CC2 level significantly better than at the CCS or SCF level.

4.3 NEON AND ARGON

Tables 8 and 9 list the results of CCSD calculations on the neon and argon atoms for dc Kerr effect, degenerate four wave mixing (DFWM), electric field induced second harmonic generation (ESHG) and third harmonic generation (THG) in the frequency range ω = 0.0 – 0.1 au or λ = 455.6 nm – ∞. From these four optical processes, the electric field induced second harmonic generation (ESHG) is of particlar interest, since for this process accurate experimental data is available from the work of Shelton and coworkers [6, 12, 40, 53, 54], which

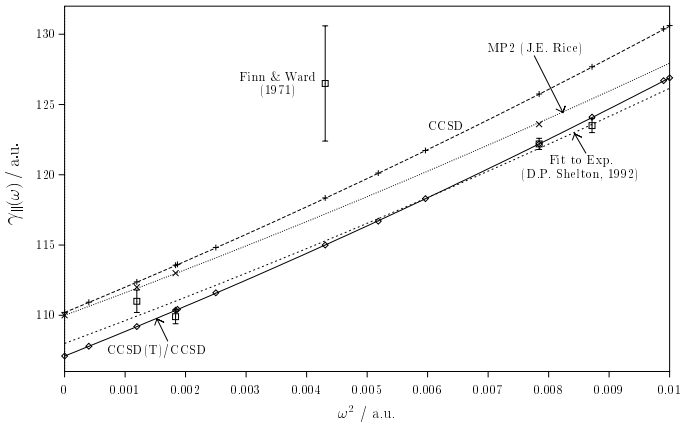


Figure 2: Electric field induced second harmonic generation in neon. Comparison of the CCSD and the CCSD(T)/CCSD curves with the experimental results [6, 12, 58] and the CCSD(T)/MP2 dispersion curve of J. E. Rice [40, 56, 57]. From Ref. [44]

covers a broad range of wavelengths between 1319 nm and 457.9 nm. Detailed plots for ESHG in Ne and Ar are shown in Figures 2 and 3. The ESHG hyperpolarizability of Ne and its static limiting value has been the subject of numerous ab initio calculations and several experimental investigations. The "ups" and "downs" of the theoretical and experimental estimates for $\gamma_0^{\rm Ne}$ can be found in recent reviews by Bishop [55] and Shelton and Rice [40]. After the latest experimental reinvestigation by Shelton and Donley [12], ESHG measurements at four frequencies were presumed to be accurate within $\pm$0.4 – 0.8 au. A fit of these four points to $\gamma_{||}^{ESHG}(\omega) = \gamma_0(1+6A\omega^2+36B\omega^4)$, where B was constraint to 5.50 au (a value arbitrary chosen between the results of a MP2 [56, 57] and a CASSCF [11] calculation) led to the estimate for the static limiting value $\gamma_0^{\rm Ne}$ = 108.1$\pm$2.2 au. However, the dispersion curve obtained by this fit does not overlap with the error bars of the two ESHG measurements in the infrared at 1319 nm and 1064 nm, as is seen in Figure 2. Thus, it was clear that at least one of these two measurements had a larger inaccuracy than indicated by its statistical uncertainty. Because of the difficulties to extrapolate from the experimental data to the static limit based on a fitted dispersion function, it was recently suggested [13] to use the dispersion curve from a CCSD response calculation, shifted such that it matches the two points measured in the visible to extrapolate to the static limit.

This extrapolation lead to the refined estimate $\gamma_0^{\rm Ne} = 106.4 \pm 2$ au. Furthermore it showed that the ESHG experiment at 1056 nm is in good agreement with the

Table 9: Dispersion curves for different optical processes for $\gamma_{||}$ of Ar, calculated at the CCSD level using the t-aug-cc-pV5Z basis.

λ/nm	ω/au	Kerr[a]	DFWM	ESHG	THG
∞	.000000	1178	1178	1178	1178
2278.2	.020000	1184	1189	1195	1212
1319.0	.034544	1195	1212	1229	1282
1064.0	.042823	1204	1230	1257	1343
1055.0	.043188	1204	1231	1258	1346
911.3	.050000	1213	1250	1287	1412
694.3	.065625	1239	1305	1376	1626
632.8	.072003	1252	1334	1422	1748
590.0	.077226	1264	1360	1465	1869
514.5	.088558	1293	1426	1577	2217
488.0	.093368	1307	1458	1634	2416
455.6	.100000	1327	1508	1722	2762

[a]For the dc Kerr effect the table lists γ_K. For the definition of γ_K see Sec. 4.

CCSD dispersion curve and the ESHG experiments at 514.5 and 488.0 nm, but that the value measured at 1319 nm is too large by $\approx$ 2.4 au. The refined estimate for $\gamma_0^{\rm Ne}$ differs from the static unrelaxed CCSD result by 3.8 au. However, this result was obtained using a frozen core approximation and the t-aug-cc-pV5Z basis. If the core electrons are correlated and the effects of connected triples are included by means of a CCSD(T) finite field calculation, one obtains for the static hyperpolarizability of neon in the t-aug-cc-pCV5Z basis $\gamma_0^{\rm Ne}$ = 107.1 au, in good agreement with the above estimate. If one accounts for these small additional basis set and correlation effects by a multiplicative correction $\gamma_{||}^{est}(\omega) = \gamma_{\text{t-aug-cc-pV5Z}}^{\text{CCSDresp}}(\omega) \times \gamma_{\text{t-aug-cc-pVC5Z}}^{\text{CCSD(T)}}(0)/\gamma_{\text{t-aug-cc-pV5Z}}^{\text{CCSDresp}}(0)$, one gets at the wavelengths of the three most reliable ESHG points: $\gamma_{||}^{est}(488.0\ \text{nm}) = 124.1$ au, $\gamma_{||}^{est}(514.5\ \text{nm}) = 122.2$ au and $\gamma_{||}^{est}(1064\ \text{nm}) = 110.4$ au. These results agree within 0.5% with the experimental ESHG data [5, 6, 12]: $\gamma_{||}^{exp}(488.0\ \text{nm}) = 123.5\pm0.5$ au, $\gamma_{||}^{exp}(514.5\ \text{nm}) = 122.2\pm0.4$ au and $\gamma_{||}^{exp}(1064\ \text{nm}) = 109.9\pm0.5$ au. To the best of our knowledge, this was the first time that for a frequency-dependent hyperpolarizability of a many-electron system agreement between theory and experiment within a 1% range could be obtained. Before this was only achieved for the two-electron systems He and H_2 [40, 59]. We note that based on the study in Sec. 4.1 remaining basis set effects can be expected to lower the

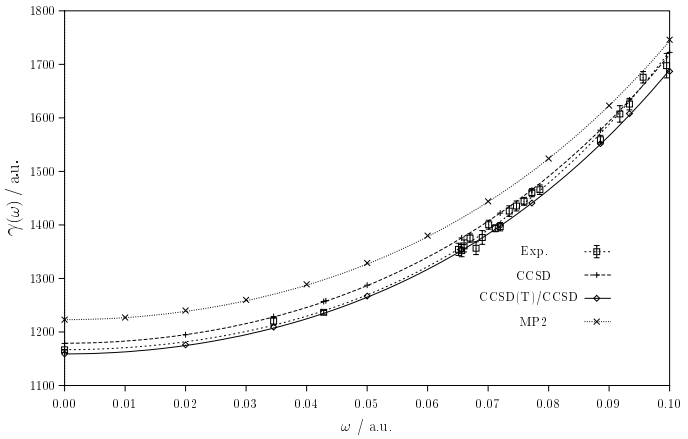


Figure 3: Electric field induced second harmonic generation in argon. Comparison of the CCSD and the CCSD(T)/CCSD response curves with the experimental results [6, 53, 54] and the CCSD(T)/MP2 dispersion curve of J. E. Rice [40, 56, 61]. The line through the experimental results is the fit of Ref. [6]. From Ref. [44]

final results. This is also indicated by a recent CCSD(T)-R12 calculation [60] for for neon which led to a value of γ_0 = 104.8 au. The remaining correlation effects (iterative triples and connected higher excitations) will in the orbital relaxed approach likely increase γ_0 slightly. Each of these effects might change $\gamma_0^{\rm Ne}$ by 1 – 3 au. In a recent DPT/MBPT-2 calculation [60] the contribution of scalar relativistic effects where calculated at the MP2 level as 3.1 au. Thus, despite of a better agreement with the experimental values one must estimate the remaining intrinsic uncertainty of the ab initio results as about $\pm$ 4 au. For argon the experimental situation is more favorable than for neon, since accurate ESHG data is available for more than 20 frequencies in the range λ = 457.9 – 1319 nm. The CCSD dispersion curve was obtained with the t-aug-cc-pV5Z basis and with only the valence electrons correlated. Even though connected triples and core effects are not considered it is already close to the fit of the experimental ESHG data. The CCSD response result for $\gamma_0^{\rm Ar}$ is within the uncertainty of the result extrapolated from a fit to this data. Correlating in the t-aug-cc-pV5Z basis all electrons gives in an unrelaxed CCSD calculation $\gamma_0^{\rm Ar}$ = 1172 au and in an orbital relaxed CCSD(T) finite field calculation $\gamma_0^{\rm Ar}$ = 1159 au. Accounting for these additional correlation effects by a multiplicative correction of the frequency-dependent CCSD results as for neon one obtains the results shown in Figure 3. The dispersion curve has mean absolute and maximum deviations from the experimental points of 0.8 and -2.6%, respectively. For shorter wavelengths the deviations become somewhat larger. The curvature of the calculated dispersion curve is slightly smaller than that for the fit through the experimental data. This an effect of the missing contributions from connected triples and higher excitations to the dispersion of $\gamma_{||}(\omega)$, which are known to lower the first excitation energy and increase the curvature of the dispersion curve. As for neon, the remaining uncertainty of the final estimates for $\gamma_0^{\rm Ar}$ due to basis set and correlation effects are estimated to be $\approx 1 - 3\%$, although a smaller mean deviation from the experimental ESHG data is found.

Since CCSD response calculations for other optical processes do not face any additional problems, we expect that the CCSD dispersion curves for dc Kerr effect, degenerate four wave mixing and third harmonic generation have about the same accuracy as the CCSD response calculations for $\gamma_{||}^{\rm ESHG}(\omega)$. The experimental situation however, is different: Only few measurements have been published for the dc Kerr effect and third harmonic generation in neon and argon and most of the experiments have uncertainties which are much larger than those of the ESHG experiments.

The THG hyperpolarizability of neon has been measured for three different wavelengths. From these three experiments only the first measurement by Ward and New [62] who obtained at λ = 694.3 nm a value of 108$\pm$18 au is in fair agreement with the ab initio result of 123.8 au. The value obtained by Lehmeier et al. [63] at 1055 nm is with 79.7$\pm$8 au about 30% smaller than the *ab initio* value which is 113.9 au for this wavelength. The recent measurement by Li et al. [64] at 1064 nm which gave 90$\pm$45 au has a too large uncertainty to be useful for a comparison with ab initio results. For argon the findings are similar: reasonable agreement is only obtained with the experiment by Ward and New [62] at 694.3 nm which gave 1525$\pm$242 au compared to the theoretical result of 1600 au. A significant disagreement is found with the newer measurement by Lehmeier et al. [63] for 1055 nm who obtained a value of 1055$\pm$105 au compared to the *ab initio* result of 1324 au for this wavelength. Again, the recent experiment by Li et al. [64] for 1064 nm has a too large uncertainty to be useful for comparison with calculations.

For the dc Kerr effect in neon only one measurement by Buckingham and Dunmur [65] has been reported in the literature. Its value of 101$\pm$8 au measured for λ = 632.8 nm falls with its error bar below the CCSD results. From the four dc Kerr measurements for argon, good agreement is only obtained with the most recent experiment by Shelton and Palubinskas [66] at 632.8 nm. The

Table 10: Comparison of the experimental data for dc Kerr effect, ESHG and THG for N_2 with the vibrational averaged CCSD response results multiplied by the factor $\gamma^{\mathrm{CCSD(T)}}_{\text{best estimate}}(0)/\gamma^{\mathrm{CCSD\ resp}}_{\text{t-aug-cc-pVTZ}}(0)$ to account approximately for connected triples and remaining basis set effects (see text for details).

	$\gamma^{ESHG}_{\|\|}(\omega)$		$\gamma^{THG}_{\|\|}(\omega)$	
λ/nm	CCSD	Exp.[a]	CCSD	Exp.
1055.0	949.8		1010.8	954 ± 95[b]
694.3	1031.2	1057.6 ± 6.4	1201.3	1295 ± 206[c]
632.8	1063.1	1095.6 ± 4.6	1283.6	
590.0	1092.7	1132.0 ± 4.2	1363.4	
514.5	1169.2	1208.7 ± 6.2	1589.2	
488.0	1207.7	1253.3 ± 6.3	1714.0	
457.9	1262.8	1327.5 ± 14.3	1907.5	

[a]References [53, 54]. [b]Reference [63]. [b]Reference [62].

earlier experiment by Buckingham and Dunmur [65] for the same wavelength is also in agreement with the CCSD calculations, but has a large uncertainty. The experimental results for 514.4 and 457.9 nm fall both with their error bars below the CCSD dispersion curve.

4.4 NITROGEN

The analysis of the calculations for Ne and Ar shows that by combination of CCSD response calculations with large correlation consistent basis sets and estimates for connected triples and core correlation it is possible to obtain for atoms agreement with the ESHG experiments within a few percents. To reach a similar accuracy for molecules is much more demanding. For a direct comparison with the experimental data, one must in addition account for vibrational averaging and for the pure vibrational and rotational contributions to the hyperpolarizabilities.

For the diatomic example N_2, the pure vibrational and rotational contributions to the ESHG process were estimated by Shelton [6]. From his work a fit through the experimental ESHG data is available which was corrected for these contributions and can directly be compared with the vibrational averaged electronic hyperpolarizabilities. Vibrational averaging has for N_2 only a small effect of $\approx$1% on γ_0 which increases slowly with the frequency. Therefore a vibrational averaging was only performed for the static limit and the two wavelengths 694.3 and 457.9 nm. For these calculations a CCSD(T)/t-aug-cc-pVTZ potential energy curve and CCSD hyperpolarizabilities for the same basis set at seven internuclear distances were used. For the remaining frequencies the zero point vibrational correction was interpolated using the expression [67] $\Delta\gamma^{ZPVA}_{||}(\omega_0;\omega_1,\omega_2,\omega_3) \approx \Delta\gamma^{ZPVA}_0(1+a\omega_L^2+b\omega_L^4)$ with $\omega_L^2=\omega_0^2+\omega_1^2+\omega_2^2+\omega_3^2$. The parameters a and b were determined by a least square fit to the points at 694.3 and 457.9 nm and the static limit. In the static limit and for small frequencies the vibrational averaged CCSD results are in almost perfect agreement with the fit through the experimental ESHG data for the electronic contribution (see Table 10 and Figure 4). However, from the basis set study in Sec. 4.1 we know that for the t-aug-cc-pVTZ basis set, which we used for the frequency-dependent calculations, the remaining basis set error is not negligible, since the extrapolated "best estimate" for the unrelaxed CCSD basis set limit is about 36 au smaller than the t-aug-cc-pVTZ result. Combining the extrapolated unrelaxed CCSD value of 867 au with the effect of connected triples from Table 6 and including the zero point vibrational correction from the CCSD calculation, one arrives at a result of $\gamma_0^{e,\mathrm{N_2}}$ = 894 au for the static hyperpolarizability of N_2. This has to be compared with the estimate obtained by Shelton from the experimental ESHG data by extrapolation: $\gamma_{||}^{e,\mathrm{N_2}}(0)$ = 917$\pm$9 au. The deviation between the two estimates is small, only 2.5%, and probably partly due to remaining basis set effects and higher-order correlation contributions. Notwithstanding this remaining uncertainty, the comparison of the dispersion curve from the vibrational averaged calculations with the experimental ESHG data demonstrates that the CCSD response approach gives an accurate description of the dispersion contribution. First for $\lambda < 570$ nm the CCSD dispersion curve falls somewhat below the fit through the experimental data, because its curvature is slightly smaller. Again, this can be attributed to the contributions from connected triples which are not included in the frequency-dependent calculations. Connected triples tend to lower excitation energies and thus to increase the dispersion of dynamic properties. One thus obtains also for the diatomic example, N_2, good agreement with the ESHG experiments, although the remaining deviation is considerably larger than for Ne and Ar.

The third harmonic generation hyperpolarizability of N_2 has been measured by Ward and New [62] for 694.3 nm and Lehmeier et al. [63] for 1055 nm. In the former experiment the ratio $\gamma^{THG}_{\mathrm{N_2}}/\gamma^{THG}_{\mathrm{He}}$ was determined at 694.3 nm as 26.75$\pm$4.25. Using the accurate ab initio results for $\gamma^{THG}_{\mathrm{He}}$ from Bishop and Pipin [59] one ob-

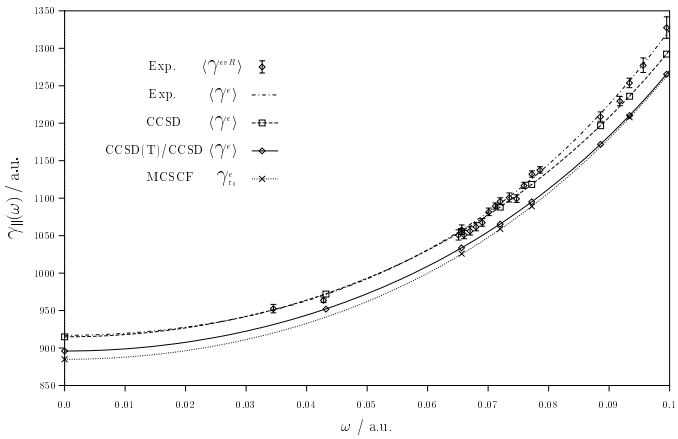


Figure 4: Electric field induced second harmonic generation in nitrogen (N_2). Comparison of the vibrational averaged CCSD and the extrapolated CCSD(T)/CCSD dispersion curves with the experimental results [6,53,54] and the MCSCF dispersion curve of Luo et al. [68]. The line through the measured points is the fit of Ref. [6] to the ESHG data after subtraction of the pure vibrational and rotational contributions.

tains $\gamma^{THG}_{N_2}(\lambda = 694.3 \text{ nm})$ = 1295±206 au. Taking into account the large uncertainty of the experimental result, this is in fair agreement with the CCSD response result, which is 1204 au (see Table 10). The vibrational and rotational contribution to $\gamma^{THG}_{N_2}(\lambda = 694.3 \text{ nm})$ were estimated by Shelton [69, 70] as -0.64 au and is thus insignificant for this comparison. Lehmeier et al. obtained for λ = 1055 nm a ratio of $\gamma^{THG}_{N_2}/\gamma^{THG}_{He}$ = 21.1±2.1, corresponding to $\gamma^{THG}_{N_2}$ = 954±95 au, which is smaller than the CCSD response result of $\gamma^{THG}_{N_2}$ = 1034.6 au and falls even below the CCSD value for the ESHG process, although the ab initio results are within the uncertainty of the experiment.

The only experimental result for the dc Kerr hyperpolarizability of N_2 is from Ref. [71] and was measured at 632.8 nm as 1443±160 au, which is much larger than the ab initio result of 949.1 au for the electronic contribution. The vibrational contribution to $\gamma_K(632.8 \text{ nm})$ was estimated in Refs. [69, 70] as 0.5 au and is thus negligible, but the rotational contribution was estimated [40] as large as 4670 au and thus hinders any meaningful comparison.

4.5 METHANE

For methane the hyperpolarizabilities were calculated at the CCSD/t-aug-cc-pVTZ level for the dc Kerr effect, ESHG and THG. For this molecule, which already has nine vibrational degrees of freedom, the vibrational contributions become substantial for the comparison with experiment. The zero point vibrational correction for $\gamma^{ESHG}_{CH_4}$ was recently calculated by Bishop and Sauer [72] using MCSCF response theory combined with a numerical differencing technique for the derivatives of γ with respect to the normal coordinates. To correct the CCSD dispersion curve for $\gamma^{ESHG}_{||}(\omega)$ we have fitted the MCSCF results of Ref. [72] to the expression $\Delta\gamma^{ZPVA}_{||}(\omega^2_L)$ = $\Delta\gamma^{ZPVA}_0(1 + a\omega^2_L + b\omega^4_L + c\omega^6_L)$. The pure vibrational contribution to $\gamma^{ESHG}_{CH_4}$ has been determined by Bishop and Pipin [73] based on the perturbational approximation introduced by Bishop and Kirtmann [74] using Hartree-Fock values for the necessary derivatives of the dipole moment, the polarizability and the first hyperpolarizability. Adding the pure vibrational contributions of Ref. [73] and the ZPVA correction to the results of the CCSD response calculation we obtained the ESHG hyperpolarizabilities in Table 11. For methane, the vibrational contributions account for $\approx$ 10 – 20% of the total hyperpolarizability. But even though these effects are treated more approximately, good agreement is obtained with the experimental ESHG results with mean absolute and maximum deviations of respectively 1.5 and 4.4%, where the largest deviation is found at 1319 nm.

To obtain more information on the remaining uncertainty of the electronic contribution, a CCSD(T)/d-aug-cc-pVTZ finite field calculation was performed which gave $\gamma^{CH_4}_{||}(0)$ = 2294 au. The unrelaxed CCSD value in the same basis is 2364 au. Thus, the sum of orbital relaxation effect and the contribution of connected triples is only small: -70 au. or -3%. Combining the best estimate of the CCSD basis set limit obtained in Sec. 4.1 with $\Delta\gamma^{ZPVA}$ and the orbital relaxation and triples effect, one gets a best estimate for the static electronic second hyperpolarizability of $\gamma^{e,CH_4}_{||}(0)$ = 2533 au. This has to be compared with experimental estimate derived from the ESHG data [6], which is 2590 au. The uncertainty of the CCSD result due to basis set incompleteness was estimated in Sec. 4.1 to be $\approx \pm 35$ au. The additional uncertainty introduced by higher-order correlation effects and the approximations used in Ref. [73] for the calculation of $\Delta\gamma^{ZPVA}$ are likely of a similar magnitude. Thus the total uncertainty of $\gamma^{e,CH_4}_{||}(0)$ is estimated to be about ± 70 au or $\pm 3\%$.

Little is known about the uncertainty of the pure vibrational contribution taken from Refs. [72, 73]. Therefore it is difficult to assess the uncertainty of the frequency-dependent results. Shelton and Palubinskas [66] have recently measured the dc Kerr hyperpolarizability for methane for seven different frequencies. To compare

Table 11: Comparison of the experimental data for dc Kerr effect, ESHG and THG in CH_4 with the ab initio calculated results which include zero point vibrational correction and the pure vibrational contribution. From Ref. [44]

λ/nm	$\gamma_K^{dcKerr}(\omega)$		$\gamma_{\|\|}^{ESHG}(\omega)$	
	CCSD	Exp.[b]	CCSD	Exp.[e]
1319.0	2894		2717	2603 ± 11
1092.0	2920[a]	2855 ± 21		
1064.0	2925		2822	2833 ± 10
763.5	3004[a]	2967 ± 16		
671.5	3054		3312	3311 ± 10
632.8	3081[a]	3070 ± 11[c]		
589.0	3120	3132 ± 27	3575	3613 ± 9
514.5	3212	3236 ± 19	3975	4060 ± 23
488.0	3256[a]	3286 ± 24		
476.5	3278		4291	4414 ± 24
457.9	3317[a]	3360 ± 14[d]		

[a]Interpolated between the calculated points. [b]Reference [66]. [c]In a previous experiment [75] at the same wavelength a value of 2887 ± 144 au was obtained. [d]In a previous experiment [76] at the same wavelength a value of 3063 ± 160 au was obtained. [e]References [6, 77].

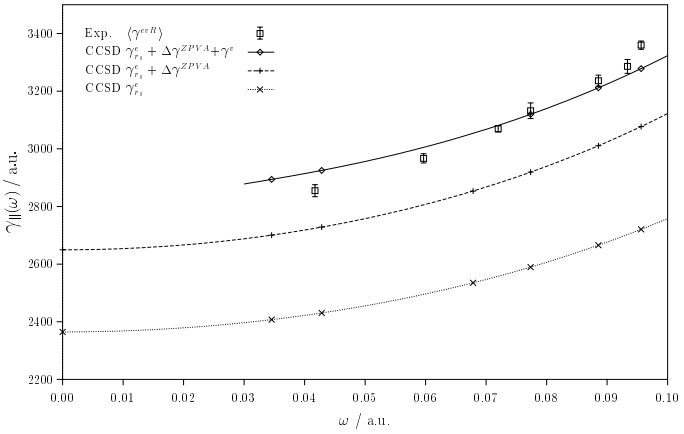


Figure 5: dc Kerr effect in methane (CH_4). Comparison of the experimental results of Ref. [66] with the CCSD response results at the equilibrium distance $\gamma^e_{r_0}$, and with the zero point vibrational corrections $\Delta\gamma^{ZPVA}$ and the pure vibrational contribution γ^v from Refs. [72, 73] added (see text for details).

the CCSD dispersion for the dc Kerr effect with the experimental results, the zero point vibrational correction was estimated from the MCRPA results for ESHG from Ref. [72], assuming that $\Delta\gamma^{ZPVA}(\omega_L^2)$ for the dc Kerr effect and ESHG follows the same dispersion curve in the effective frequency ω_L^2. Thereby one neglect the small difference between γ_K and $\gamma_{||}$ and the fact that $\Delta\gamma^{ZPVA}(\omega_L^2)$ for the dc Kerr effect and ESHG differ in sixth order in ω_L. The pure vibrational contribution is again taken from Ref. [73]. The results obtained by adding these contributions to the CCSD response values are compared with the experimental results of Shelton and Palubinskas in Figure 5.

On the average we obtain a good agreement between the calculated curve and the experimental results of Ref. [66] with deviations of only 0.5 – 2.5%. But the dispersion of the ab initio curve is distinctly too small to fit to the experimental points: for the lower frequencies the calculated results are too large by $\approx 2.5\%$, while for the higher frequencies they are too small by $\approx 2.5\%$. Although it is expected that the inclusion of connected triples in the response calculations would slightly increase the dispersion of the electronic contribution, this deviation can hardly be traced back to this effect, since the comparison of the ESHG data showed that the dispersion of the electronic hyperpolarizabilities is well described at the CCSD response level. It was already observed by Shelton and Palubinskas [66] that the calculated values for the vibrational hyperpolarizability of Ref. [73] disagreed in size and dispersion with the analysis of the experimental results. Is is therefore likely that a large fraction of the discrepancy between the ab initio dispersion curve and the Kerr measurements is a consequence of the approximations used in Ref. [73] for the calculation of the vibrational contribution. Nevertheless, this is the first time that for a dc Kerr hyperpolarizability agreement within a few percents is obtained between ab initio calculations and experimental measurements.

4.6 SULPHURHEXAFLUORIDE

Figure 6 shows the CCSD results for the dc Kerr and the ESHG hyperpolarizability of SF_6. Because for this molecule the calculation of the hyperpolarizabilities at a larger number of frequencies was prohibitive in any acceptable basis set a different approach to the frequency-dependent hyperpolarizabilities was taken. Instead of computing the frequency-dependent hyperpolarizabilities for each process at number of different frequencies, the dispersion coefficients for the electronic second hyperpolarizabilities were calculated as analytic derivatives

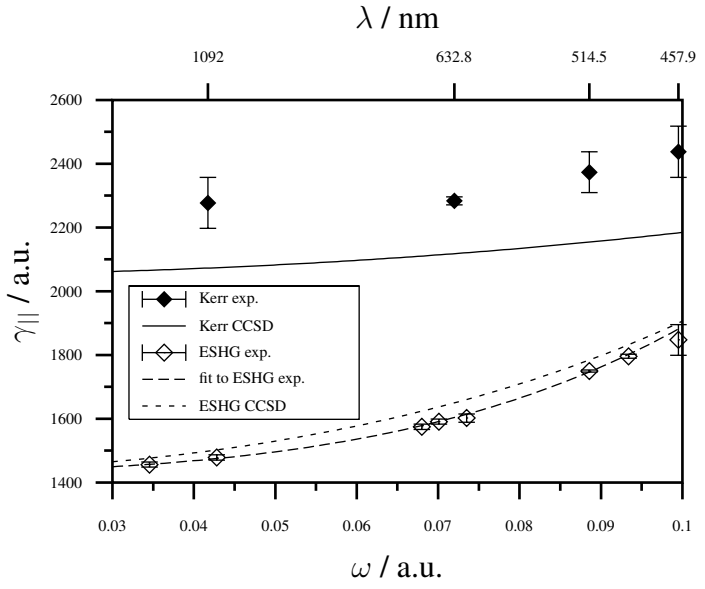


Figure 6: Electric field induced second harmonic generation and dc Kerr effect in sulphurhexafluoride (SF_6). Comparison of the experimental results of Ref. [6, 66] with the CCSD results at a S–F bond distance of 1.564 Å. The CCSD results contain the nuclear relaxation contribution from Ref. [78]. The curvature contribution is neglected.

of $\gamma(\omega_\sigma;\omega_1,\omega_2,\omega_3)$ with respect to its frequency arguments [27, 28, 79, 80] and the frequency-dependent hyperpolarizabilities were then approximated by [1,1] Padé approximants:

$$\gamma_{||}(-2\omega;\omega,\omega,0) \approx \gamma_0\Big(1+6(A-B/A)\omega^2\Big)/\Big(1-6B/A\omega^2\Big) \quad (44)$$

$$\gamma^K(-\omega;0,0,\omega) \approx \gamma_0\Big(1+2(A^K-B^K/A^K)\omega^2\Big)/\Big(1-2B^K/A^K\omega^2\Big) \quad (45)$$

The static hyperpolarizability and the coefficients A, A^K were calculated at the CCSD level in the d-aug-cc-pVTZ basis, which for SF_6 consists of 438 basis functions. To the best of our knowledge, this is still today the largest CCSD hyperpolarizability calculation carried out. The fourth-order coefficients B and B^K were calculated in a slightly smaller basis, in which the two most diffuse f-type functions at the fluorine atoms have been omitted. The numerical values of the dispersion coefficients are: γ_0 = 1506.5 au, A = 4.2071, B = 14.11, A^K = 4.16, and B^K = 13.36. Since no data was available for the zero point vibrational correction and for some of the pure vibrational contributions, only the nuclear relaxation contribution to the pure vibrational contribution calculated at the SCF level in Ref. [78] could be included. As is seen in Figure 6, nevertheless a reasonable good agreement with the experimental results is obtained for the ESHG process. For the dc Kerr effect the deviation of the *ab initio* results from the experimental data is much larger. This must be attributed to the pure vibrational contribution, which was treated rather approximately in the calculation, but makes a substantial contribution to the dc Kerr effect.

Table 12: Fifth harmonic generation in rare gas atoms calculated at the CCSD level using t-aug-cc-pV5Z basis sets (in 10^3 au).

	Atom	λ/nm	CCSD	Lit.	Exp.
He	∞		15.01	14.94[a]	
Ne	∞		60.54		
	1064		83.31		322±161[b]
Ar	∞		1868.		
	1064		3695.		1472±736[b]

[a]CI-Hylleraas, Ref. [59] [b]Ref. [64]

5 FIFTH HARMONIC GENERATION IN RARE GAS ATOMS

As mentioned in the introduction, the systematic "lego brick" like structure of the coupled cluster response theory made it possible to give an open ended formulation of the coupled cluster response functions and to implement them up to a relatively high order. This made it for the first time possible to carry out correlated *ab initio* calculations on the fifth harmonic generation (FHG) hyperpolarizabilities on systems with more than two electrons. A severe problem which appears for *ab initio* calculations of such high-order hyperpolarizabilities is that convergence with respect to the one-electron basis set became rather slow. Test calculations indicate that even with a t-aug-cc-pV5Z basis the CCSD results are not converged better than within ±2-5%. However, also the experimental determination of absolute values — i.e. not relative to a reference substance — of these high-order hyperpolarizabilities is a rather difficult task, as is obvious from the large uncertainties of the experimental results. For the fifth harmonic generation in rare gases only one experiment at 1064 nm is available. Even though the error bars are with ±50% rather large, they do not overlap with the theoretical results. For neon the experimental

result is about four times larger than the CCSD number and for argon the experimental $\epsilon_{||}^{FHG}$ is about a factor of two smaller than the CCSD result. Since for the CCSD calculations the relative error should be about the same for neon and for argon, it is expect that the experimental results are even less accurate than indicated by their uncertainties. This is also corroborated by the results for the third harmonic generation which were obtained in the same experiment and have much larger errors the *ab initio* calculations in Sec. 4.3.

6 ELECTRIC FIELD GRADIENT INDUCED BIREFRINGENCE

The electric-field-gradient induced anisotropy of the refractive index in an ideal gas is given by

$$\Delta n = n_{XX} - n_{YY} = 2\pi N q \Big\{ b(\omega) + \frac{2\Theta_{\alpha\beta}\alpha_{\alpha\beta}(\omega)}{15kT} \Big\} \tag{46}$$

where n is the refractive index, N the number density, q the electric field gradient, $\boldsymbol{\Theta}$ the permanent quadrupole moment tensor, and $\boldsymbol{\alpha}(\omega)$ the electric dipole polarizability. Eq. (46) applies to both polar and non-polar species. In latter case $\boldsymbol{\Theta}$ refers to the so-called "effective quadrupole center" as origin as discussed in detail in Refs. [81, 82].

For systems of cubic or higher point group symmetry, the orientational contribution $2\Theta_{\alpha\beta}\alpha_{\alpha\beta}(\omega)/15kT$ vanishes, and the observed anisotropy reduces to

$$\Delta n = 2\pi \; N \; q \; b(\omega) \tag{47}$$

The contribution $b(\omega)$ — the temperature-independent term — is a combination of three hyperpolarizabilities [81, 83]

$$\begin{aligned} b(\omega) &= \frac{2}{15}[B_{\alpha,\beta,\alpha\beta}(-\omega;\omega,0) - B_{\alpha,\beta,\alpha\beta}(-\omega;0,\omega)] \\ &\quad -\frac{2}{3\omega}\epsilon_{\alpha\beta\gamma}J_{\alpha\beta\gamma}(-\omega;\omega,0) \end{aligned} \tag{48}$$

where $\epsilon_{\alpha\beta\gamma}$ is the Levi-Civita tensor and B and J in terms of response functions are given by [84]

$$B_{\alpha,\beta,\gamma\delta}(-\omega_\sigma;\omega_1,\omega_2) = \langle\langle \hat{\mu}_\alpha; \hat{\mu}_\beta, \hat{\Theta}_{\alpha\beta}\rangle\rangle_{\omega_1,\omega_2} \; , \tag{49}$$

$$J_{\alpha\beta\gamma}(-\omega_\sigma;\omega_1,\omega_2) = i\langle\langle \hat{\mu}_\alpha; \hat{m}_\beta, \hat{\mu}_\gamma\rangle\rangle_{\omega_1,\omega_2} \; . \tag{50}$$

In the above equations $\hat{\mu}$, $\hat{\Theta}$ and $\hat{m}$ are the electric dipole, electric quadrupole and magnetic dipole operators, respectively, and $\omega_\sigma = \omega_1 + \omega_2$.

The frequency dependence of $b(\omega)$ can be obtained through the dispersion coefficients for the individual hyperpolarizability contributions. As discussed in Ref. [85], quadratic response functions for a finite molecular or atomic system in its electronic ground state are analytic in the frequency arguments, except at the poles. Due to the matching condition between the frequencies of the response function, $\sum_i \omega_i = 0$, only two of the three frequency arguments are independent and the quadratic response function can be expanded in Taylor series as

$$\langle\langle A; B, C\rangle\rangle_{\omega_B,\omega_C} = \sum_{n,m=0}^{\infty} \omega_B^n \, \omega_C^m \, D_{ABC}(n,m) \; . \tag{51}$$

In Ref. [85] analytical expressions for the expansion (dispersion) coefficients $D_{ABC}(n,m)$ were derived for a general coupled cluster quadratic response function. It was shown that the coefficients with even total order $n+m$ are real, while those with odd total order $n+m$ are pure imaginary. Thus when the (hermitian) operators A, B and C are real, the expansion contains only terms of even total order, whereas if exactly one of the operators is pure imaginary, only odd terms are present. For the hyperpolarizabilities B and J entering $b(\omega)$ one of the two frequencies is zero, and the expansion is analogous to that of the first electric dipole hyperpolarizability $\beta_{\alpha\beta\gamma}(-\omega,\omega,0)$ describing the electro-optical Pockels effect (see Eq. (44) in Ref. [85]):

$$B_{\alpha,\beta,\gamma\delta}(-\omega,\omega,0) = \sum_{n=0}^{\infty} \omega^{2n} B_{\alpha,\beta,\gamma\delta}(2n) \tag{52}$$

$$\begin{aligned} B_{\alpha,\beta,\gamma\delta}(-\omega,0,\omega) &= B_{\alpha,\gamma\delta,\beta}(-\omega,\omega,0) \\ &= \sum_{n=0}^{\infty} \omega^{2n} B_{\alpha,\gamma\delta,\beta}(2n) \end{aligned} \tag{53}$$

$$J_{\alpha\beta\gamma}(-\omega,\omega,0) = \sum_{n=0}^{\infty} \omega^{2n+1} J_{\alpha\beta\gamma}(2n+1) \tag{54}$$

The odd-order expansion for J is due to the imaginary nature of the magnetic dipole operator. At zero frequency the two dipole-dipole-quadrupole contributions cancel each other. The resulting dispersion formula for $b(\omega)$, Eq. 48, can thus be written as:

$$b(\omega) = \sum_{n=0}^{\infty} \omega^{2n} \, b(2n) \tag{55}$$

with

$$b(2n) = \begin{cases} -\frac{2}{3}\epsilon_{\alpha\beta\gamma}J_{\alpha\beta\gamma}(1) & \text{for} \quad n=0 \\ -\frac{2}{3}\epsilon_{\alpha\beta\gamma}J_{\alpha\beta\gamma}(2n+1) & \text{for} \quad n>0 \\ +\frac{2}{15}\Big[B_{\alpha,\beta,\alpha\beta}(2n) - B_{\alpha,\alpha\beta,\beta}(2n)\Big] & \end{cases} \tag{56}$$

For atoms the tensors B and J are determined each by a single constant [81]

$$B_{\alpha,\beta,\gamma\delta} = B\Big[-\frac{1}{2}\delta_{\alpha\beta}\delta_{\gamma\delta}+\frac{3}{4}(\delta_{\alpha\gamma}\delta_{\beta\delta}+\delta_{\alpha\delta}\delta_{\beta\gamma})\Big], \quad (57)$$

$$J_{\alpha\beta\gamma} = J\epsilon_{\alpha\beta\gamma} \quad (58)$$

and $b(\omega)$ reduces to

$$b(\omega) = B(-\omega;\omega,0) - B(-\omega;0,\omega) - \frac{4}{\omega}J(-\omega;\omega,0)\ . \quad (59)$$

For easiness of notation we will use in the following the symbol $\mathcal{B}$ for the $B(-\omega;0,\omega)$ hyperpolarizability of atoms and its dispersion coefficients, reserving B to $B(-\omega;\omega,0)$ and its dispersion coefficients.

For atoms — similar as the paramagnetic hypermagnetizability contribution to the Cotton-Mouton constant [86, 87]— the hyperpolarizability $J(-\omega_\sigma;\omega_1,\omega_2)$ can be expanded in a power series in the frequencies ω_1 and ω_2 using the Cauchy moments: [88]

$$\begin{aligned} J_{xyz}(-\omega_\sigma;\omega_1,\omega_2) &= \frac{1}{2}\sum_{n=0}^{\infty} S(-2n-4) \quad (60)\\ &\times \sum_{m=0}^{2n+1} \omega_1^{2n+1-m}\,\omega_2^m \begin{pmatrix} 2n+2 \\ m \end{pmatrix}\ . \end{aligned}$$

For the dipole-dipole-magnetic dipole hyperpolarizability $J(-\omega;\omega,0)$, which enters the dominant contributions to the temperature-independent term in EFGB, Eq. (60) reduces to:

$$\begin{aligned} J_{xyz}(-\omega;\omega,0) &= \frac{1}{2}\sum_{n=0}^{\infty}\omega^{2n+1}\,S(-2n-4) \quad (61)\\ &= \frac{1}{2\omega}\Big[\alpha(\omega)-\alpha(0)\Big] \quad (62) \end{aligned}$$

and the dispersion coefficients for the expansion of $b(\omega)$ in Eq. (55) for atoms simply become

$$b(2n) \;=\; B(2n) - \mathcal{B}(2n) - 2S(-2n-4) \quad (63)$$

6.1 COMPUTATIONAL DETAILS

For the three atoms He, Ne and Ar a basis set investigation was performed at the experimental frequency using the doubly augmented correlation consistent sets [89,90] d-aug-cc-pVXZ, with X=Q, 5 and 6 for He and X=T, Q and 5 for Ne and Ar. For Ne calculations were also carried out with the core-valence correlation consistent set d-aug-cc-pCVQZ. [35, 91] Only the d-aug-cc-pVDZ set was employed for the calculations on sulphurhexafluoride.

Table 13: Helium, Neon and Argon. Hyperpolarizability contributions and total $b(\omega)$ at 632.8 nm (au).

Basis	B	$\mathcal{B}$[a]	J	b
Helium, FCI				
d-aug-cc-pVQZ	-7.449	-7.407	0.056	-3.161
aug-cc-pV5Z	-6.428	-6.379	0.056	-3.148
d-aug-cc-pV5Z	-7.477	-7.435	0.056	-3.156
t-aug-cc-pV5Z	-7.475	-7.433	0.056	-3.155
d-aug-cc-pV6Z	-7.457	-7.415	0.056	-3.152
Neon, CCSD				
d-aug-cc-pVTZ	-14.975	-14.899	0.106	-5.991
d-aug-cc-pVQZ	-16.204	-16.122	0.105	-5.928
d-aug-cc-pV5Z	-17.431	-17.356	0.105	-5.885
Argon, CCSD				
d-aug-cc-pVTZ	-151.91	-150.00	1.031	-59.19
d-aug-cc-pVQZ	-154.62	-152.84	1.014	-58.10
d-aug-cc-pV5Z	-159.02	-157.37	1.014	-58.01

[a] $\mathcal{B} = B(-\omega,0,\omega)$.

The dispersion coefficients were calculated for each system for the largest (valence only) basis set. Note that the CCSD results for He are full configuration interaction (FCI) results. For Ar and SF_6 only the valence electrons were correlated, while for Ne the d-aug-cc-pCVQZ calculations were carried out with all electrons correlated. For SF_6 again a S−F bond distance of 1.564 Å was employed.

For all calculations a local version of the DALTON program package [46] was employed which included the integral-direct Coupled Cluster response program. [18, 22, 23, 26, 27, 92]

6.2 HELIUM, NEON AND ARGON

Table 13 lists the results for the unique components of the hyperpolarizabilities B, $\mathcal{B}$ and J, and the total anisotropy $b(\omega)$ at 632.8 nm. For helium, J and b show a monotonic convergence trend when increasing the ζ-level X of the basis set, although the hyperpolarizabilities B and $\mathcal{B}$ behave somewhat unsystematic with the basis set. Due to cancellation, however, the net effect of the anisotropy $B-\mathcal{B}$ is monotonic. The non-monotonic behavior of B and $\mathcal{B}$ of helium with increasing zeta level, which is opposite to what is observed for neon and argon, might be an effect of the different construc-

Table 14: Helium, Neon, and Argon. Frequency dispersion coefficients (au).

n	$B(2n)$	$\mathcal{B}(2n)$[a]	$S(-2n-4)$	$b(2n)$
Helium, FCI/d-aug-cc-pV6Z,				
0	-7.338427	-7.338427	1.54397	-3.08794
1	-22.61413	-14.54661	2.04567	-12.1589
2	-54.64730	-26.88535	2.92777	-33.6175
3	-120.7737	-48.22812	4.37633	-81.2983
Neon, CCSD/d-aug-cc-pV5Z, $1s^2$ frozen				
0	-17.12136	-17.12136	2.87891[b]	-5.75782
1	-58.72559	-44.63564	5.00637[b]	-24.1027
2	-175.0149	-121.0321	10.6895[b]	-75.3618
3	-495.6875	-337.9173	25.1286[b]	-208.027
Argon, CCSD/d-aug-cc-pV5Z, $1s^22s^22p^6$ frozen				
0	-152.9822	-152.9822	27.6880[c]	-55.3760
1	-1128.719	-828.1085	92.6903[c]	-485.991
2	-6884.157	-4372.971	374.429[c]	-3260.04
3	-38331.59	-23631.67	1688.32[c]	-18076.6

[a] $\mathcal{B}(2n)$ are the dispersion coefficients for $B(-\omega, 0, \omega)$. [b] CCSD/q-aug-cc-pV5Z/all electrons correlated: [26] 2.857, 4.949, 10.54, 24.73; DOSD: [93] 2.886, 5.063, 10.86, 25.53. [c] DOSD: [93] 27.91, 95.06, 391.5 , 1802.

tion schemes for the diffuse functions of helium in the aug-cc-pVXZ basis sets. [89] For neon the convergence of the two dipole-dipole-quadrupole hyperpolarizabilities is monotonic, while the total anisotropy $B-\mathcal{B}$ is not. This does not, however, affect the convergence trend for $b(\omega)$. Deviation from a monotonic behavior is observed also for J of argon, but again without effect on the final $b(\omega)$. The variation between d-aug-cc-pV5Z and d-aug-cc-pV6Z results for $b(\omega)$ of helium is ca. 0.004 au. To assess the inaccuracy of the calculated $b(\omega)$ due to basis set incompleteness we have also analyzed the effect of multiple augmentation for the X=5 polarization level. As expected, double augmentation is found to give the largest variation, ca 0.007 au, while the effect of triple augmentation is an order of magnitude smaller. From these results it is expected that the true values for $b(\omega)$ at 632.8 nm are about -3.15 ± 0.01 au.

To estimate the correlation effects beyond CCSD for Ne and Ar, calculations were carried out in the d-aug-cc-pV5Z basis set for the hierarchy CCS, CC2 and CCSD. For Ne, the results for $b(\omega)$ at 632.8 nm are: -4.349 au (CCS), -5.941 au (CC2), and -5.885 au (CCSD). Thus, the CC2 result for $b(\omega)$ is, in absolute value, larger than the CCSD result, the difference being ca. 0.06 au. Higher excitation effects are expected to be smaller, which is corroborated by results obtained for the static polarizability of neon by Christiansen et al. [94], and the connection between $b(\omega)$ and α of atoms discussed in Sec. 6. To estimate the core correlation effect for neon an additional calculation was carried out in the d-aug-cc-pCVQZ basis set with all electrons correlated. At the CCSD level the result for $b(\omega)$ and 632.8 nm is -5.858 au. From the difference of the d-aug-cc-pVQZ/frozen core and the of d-aug-cc-pCVQZ/all-electron result one thus obtains a core correlation effect of $+0.07$ au. For argon, the behavior of the calculated $b(\omega)$ in the CC hierarchy is completely monotonic: -53.379 au (CCS), -57.158 au (CC2) and -58.012 au (CCSD). The difference between CC2 and CCSD is 0.85 au. Again, the contributions from higher excitation levels are expected to be at most of the same order of magnitude. Since in the calculations on neon the core correlation effect turned out to be negligible, it was not determined for argon.

Thus, with conservative estimates for the uncertainties caused by remaining higher-order correlation and basis set effects, one arrives at best estimates for $b(632.8\mathrm{nm})$ of Ne and Ar of -5.9 ± 0.1 au and -58 ± 2 au, respectively. This expectation is supported by the good agreement obtained between the CCSD values for the Verdet constant and the experimental results for this property. [88] Experimental results for the EFGB of helium and neon are not available in the literature. The EFGB of Ar at 632.8 nm was measured 1968 by Buckingham, Dish and Dunmur, [95] and $b(\omega)$ was found to be 0 ± 109 au.

As shown in section 6, the dipole-dipole-magnetic dipole hyperpolarizability J for atoms is related to the difference between the frequency-dependent and the static dipole polarizability. This means that the dispersion coefficients $J(n)$ are simple multiples of the Cauchy moments. The latter are therefore collected in Table 14 together with the dispersion coefficients for the two hyperpolarizabilities B and $\mathcal{B}$, and those for $b(\omega)$.

Buckingham and Jamieson [83] were the first to establish the connection between the zero-frequency limit of $b(\omega)$ and the Verdet constant for atoms

$$\lim_{\omega\to 0} b(\omega) = -C \lim_{\omega\to 0} \frac{V(\omega)}{\omega^2} \tag{64}$$

where C is the appropriate dimensional constant. According to our expansion for b and V, Eq. (64) becomes:

$$b(0) = -CV(2). \tag{65}$$

Table 15: SF_6. Symmetry-unique hyperpolarizability contributions and total $b(\omega)$ at 632.8 nm (au). CCSD/d-aug-cc-pVDZ/frozen core.

$B_{z,z,zz}$	-231.4842
$B_{x,z,xz}$	-230.6594
$B_{z,zz,z}$	-229.5050
$B_{x,xz,z}$	-229.5207
J_{xyz}	1.68005
$b^{a,b}$	-95.03517

[a] $b(\omega) = \frac{2}{5}[B_{z,z,zz} - B_{z,zz,z} + 2(B_{x,z,xz} - B_{x,xz,z})] - 4\omega^{-1}J_{xyz}$.
[b] Experiment: [95] $b = 0 \pm 109$ au.

From this relationship, Buckingham and Jamieson [83] estimated $b(0)$ for the three rare gases considered here from values of the zero frequency limit of $V(\omega)/\omega^2$. For He the latter were taken from a variational calculation of Victor, Dalgarno and Taylor. [96] For Ne and Ar, they were derived from the expressions for V of Dalgarno and Kingston. [97] The resulting estimates were $b(0) = -3.06$ au for He, $b(0) = -5.75$ au for Ne, and $b(0) = -54.90$ au for Ar, in rather good agreement with our $b(0) = -3.088$ au for He, $b(0) = -5.758$ au for Ne, and $b(0) = -55.376$ au for Ar respectively.

6.3 SULPHURHEXAFLUORIDE SF_6

The results for the symmetry unique components of the hyperpolarizabilities entering the EFGB and of the final $b(\omega)$ at the experimental frequency are collected in Table 15. At 632.8 the value of $b(\omega)$ is -95 au. However, the quality of the only experimental result [95] available in the literature is rather poor and not very helpful for comparison with the theoretical result: 0 ± 109 au. Even though the calculated result was obtained with a relatively small basis set and does not include any vibrational corrections, it can serve as indication for a new experimental determination of the electric-field-induced birefringence of SF_6.

7 SUMMARY

The recent developments in coupled cluster nonlinear response theory, which led to the implementation of the quadratic through quintic response functions for the coupled cluster models CCS, CC2, and CCSD and the quadratic response function for CC3, made it possible to carry out *ab initio* calculations of frequency-dependent high-order properties on a level which accounts efficiently and accurately for dynamic electron correlation. At the CCSD level one reaches for the first time an accuracy for the dispersion of frequency-dependent properties which makes it possible to calculate (and predict) nonlinear optical and magneto-optical properties within a few percent. To reach such an accuracy in practice for molecules is, however, still a very difficult task which requires rather expansive calculations. At least for small molecules basis sets of quadruple-ζ or better quality need to be used. The inclusion of the zero point vibrational correction and the pure vibrational contributions are mandatory and at least in the static limit the effect of connected triple excitations need to be included. To reach an accuracy of 1 – 2% also core correlation and relativistic effects must be included.

References

[1] D. N. Zubarev, Usp. Fiz. Nauk (English translation Soviet Phys. Uspekhi 3 (1960) 320. **71** (1960).

[2] J. Linderberg and Y. Öhrn, Proc. Roy. Soc. (London) A. **285**, 445 (1965).

[3] Y. Öhrn and J. Linderberg, Phys. Rev. A. **139**, 1063 (1965).

[4] J. Linderberg and Y. Öhrn. *Propagators in Quantum Chemistry*. Academic, London, 1973.

[5] D. P. Shelton, Phys. Rev. Lett. **62**, 2660 (1989).

[6] D. P. Shelton, Phys. Rev. A. **42**, 2578 (1990).

[7] D. P. Shelton and Z. Lu, Phys. Rev. A. **37**, 2231 (1988).

[8] D. P. Shelton and Z. Lu, Phys. Rev. A. **37**, 3813 (1988).

[9] M. Jaszuński and D. L. Yeager, Phys. Rev. A. **40**, 1651 (1989).

[10] D. M. Bishop, Phys. Rev. Lett. **65**, 1688 (1990).

[11] H. J. A. Jensen, P. Jørgensen, H. Hettema and J. Olsen, Chem. Phys. Lett. **187**, 387 (1991).

[12] D. P. Shelton and E. A. Donley, Chem. Phys. Lett. **195**, 591 (1992).

[13] C. Hättig and P. Jørgensen, Chem. Phys. Lett. **283**, 109 (1998).

[14] O. Christiansen, P. Jørgensen and C. Hättig, Int. J. Quantum Chem. **68**, 1 (1998).

[15] J. Olsen and P. Jørgensen. *Time-Dependent Response Theory with Applications to Self-Consistent Field and Multiconfigurational Self-Consistent Field Wave Functions*, in *Modern Electronic Structure Theory*, edited by D. R. Yarkony, volume 2, chapter 13, pp. 857–990. World Scientific, Singapore, 1995.

[16] H. Sambe, Phys. Rev. A. **7**, 2203 (1972).

[17] P. W. Langhoff, S. T. Epstein and M. Karplus, Rev. Mod. Phys. **44**, 602 (1972).

[18] C. Hättig, O. Christiansen, H. Koch and P. Jørgensen, Chem. Phys. Lett. **269**, 428 (1997).

[19] C. Hättig, O. Christiansen and P. Jørgensen, Chem. Phys. Lett. **282**, 139 (1998).

[20] C. Hättig, O. Christiansen and P. Jørgensen, J. Chem. Phys. **108**, 8331 (1998).

[21] H. Koch, O. Christiansen, R. Kobayashi, P. Jørgensen and T. Helgaker, Chem. Phys. Lett. **228**, 233 (1994).

[22] A. Halkier, H. Koch, O. Christiansen, P. Jørgensen and T. Helgaker, J. Chem. Phys. **107**, 849 (1997).

[23] O. Christiansen, A. Halkier, H. Koch, P. Jørgensen and T. Helgaker, J. Chem. Phys. **108**, 2801 (1998).

[24] C. Hättig, O. Christiansen and P. Jørgensen, J. Chem. Phys. **108**, 8355 (1998).

[25] C. Hättig, O. Christiansen, S. Coriani and P. Jørgensen, J. Chem. Phys. **109**, 9237 (1998).

[26] C. Hättig, O. Christiansen and P. Jørgensen, J. Chem. Phys. **107**, 10592 (1997).

[27] C. Hättig and P. Jørgensen, Theor. Chim. Acc. **100**, 230 (1998).

[28] C. Hättig and P. Jørgensen, Advances in Quantum Chemistry. **35**, 111 (1999).

[29] S. Coriani, C. Hättig, P. Jørgensen and T. Helgaker, J. Chem. Phys. **113**, 3561 (2000).

[30] T. Helgaker, H. J. Å. Jensen, P. Jørgensen, J. Olsen, K. Ruud, H. Ågren, A. A. Auer, K. L. Bak, V. Bakken, O. Christiansen, S. Coriani, P. Dahle, E. K. Dalskov, T. Enevoldsen, B. Fernandez, C. Hättig, K. Hald, A. Halkier, H. Heiberg, H. Hettema, D. Jonsson, S. Kirpekar, R. Kobayashi, H. Koch, K. V. Mikkelsen, P. Norman, M. J. Packer, T. B. Pedersen, T. A. Ruden, A. Sanchez, T. Saue, S. P. A. Sauer, B. Schimmelpfennig, K. O. Sylvester-Hvid, P. R.Taylor, and O.Vahtras. Dalton – an electronic structure program, release 1.2, 2001.

[31] J. Gauss, O. Christiansen and J. F. Stanton, Chem. Phys. Lett. **296**, 117 (1998).

[32] J. Dudley and J. Ward, J. Chem. Phys. **82**, 4673 (1985).

[33] H. Sekino and R. J. Bartlett, J. Chem. Phys. **84**, 2726 (1986).

[34] H. Larsen, J. Olsen, C. Hättig, P. Jørgensen, O. Christiansen and J. Gauss, J. Chem. Phys. **111**, 1917 (1999).

[35] T. H. Dunning, J. Chem. Phys. **90**, 1007 (1989).

[36] R. A. Kendall, T. H. Dunning and R. J. Harrison, J. Chem. Phys. **96**, 6796 (1992).

[37] D. E. Woon and T. H. Dunning, J. Chem. Phys. **98**, 1358 (1993).

[38] D. E. Woon and T. H. Dunning, J. Chem. Phys. **100**, 2975 (1994).

[39] A. K. Wilson, D. E. Woon, K. A. Peterson and T. H. Dunning, J. Chem. Phys. **110**, 7667 (1999).

[40] D. P. Shelton and J. E. Rice, Chem. Rev. **94**, 3 (1994).

[41] I. J. Bigio and J. F. Ward, Phys. Rev. A. **9**, 35 (1974).

[42] K. P. Huber and G. Herzberg. *Molecular Spectra and Molecular Structure: IV. Constants of Diatomic Molecules*. Van Nostrand, New York, 1979.

[43] D. L. Gray and A. G. Robiette, Mol. Phys. **37**, 1901 (1979).

[44] C. Hättig and P. Jørgensen, J. Chem. Phys. **109**, 2762 (1998).

[45] P. Norman, D. Jonsson, O. Vahtras and H. Ågren, Chem. Phys. **203**, 23 (1996).

[46] T. Helgaker, H. J. Å. Jensen, P. Jørgensen, J. Olsen, K. Ruud, H. Ågren, T. Andersen, K. L. Bak, V. Bakken, O. Christiansen, P. Dahle, E. K. Dalskov, T. Enevoldsen, B. Fernandez, H. Heiberg, H. Hettema, D. Jonsson, S. Kirpekar, R. Kobayashi, H. Koch, K. V. Mikkelsen, P. Norman, M. J. Packer, T. Saue, P. R. Taylor, and O. Vahtras. Dalton – an electronic structure program, release 1.0, 1997.

[47] D. E. Woon and T. H. Dunning, J. Chem. Phys. 103, 4572 (1995). The basis sets were obtained from the Extensible Computational Chemistry Environment Basis Set Database, Version 1.0, as developed and distributed by the Molecular Science Computing Facility, Environmental and Molecular Sciences Laboratory which is part of the Pacific Northwest Laboratory, P.O. Box 999, Richland, Washington 99352, USA, and funded by the U.S. Department of Energy. PNL is a multiprogram laboratory operated by Batelle Memorial Institute for the U.S. Department of Energy under contract DE-AC06-76RLO 1830.

[48] J. Stiehler and J. Hinze, J. Phys. B. **28**, 4055 (1995).

[49] E. A. Salter, H. Sekino and R. J. Bartlett, J. Chem. Phys. **87**, 502 (1987).

[50] R. Kobayashi, H. Koch, P. Jørgensen and T. J. Lee, Chem. Phys. Lett. **211**, 94 (1993).

[51] C. Hättig and B. A. Heß, Chem. Phys. Lett. **233**, 359 (1995).

[52] J. E. Rice and N. C. Handy, Int. J. Quantum Chem. **43**, 91 (1992).

[53] Y. Mizrahi and D. P. Shelton, Phys. Rev. Letters. **55**, 696 (1985).

[54] Y. Mizrahi and D. P. Shelton, Phys. Rev. A. **31**, 3145 (1985).

[55] D. M. Bishop, Adv. Quant. Chem. **25**, 2 (1994).

[56] J. E. Rice, J. Chem. Phys. **96**, 7580 (1992).

[57] J. E. Rice, G. E. Scuseria, T. Lee, P. R. Taylor and J. Almlöf, Chem. Phys. Lett. **191**, 23 (1992).

[58] R. S. Finn and J. F. Ward, Phys. Rev. Lett. **26**, 285 (1971).

[59] D. M. Bishop and J. Pipin, J. Chem. Phys. **91**, 3549 (1989).

[60] R. Franke, H. Müller and J. Noga, J. Chem. Phys. **114**, 7746 (2001).

[61] J. E. Rice, P. R. Taylor, T. J. Lee and J. Almlöf, J. Chem. Phys. **94**, 4972 (1991).

[62] J. F. Ward and G. H. C. New, Phys. Rev. **185**, 57 (1969).

[63] H. J. Lehmeier, W. Leupacher and A. Penzkofer, Opt. Coummun. **56**, 67 (1985).

[64] X. F. Li, A. L'Huillier, M. Ferray, L. A. Lompré and G. Mainfray, Phys. Rev. A. **39**, 5731 (1989).

[65] A. D. Buckingham and D. A. Dunmur, Trans. Faraday Soc. **64**, 1776 (1968).

[66] D. P. Shelton and J. J. Palubinskas, J. Chem. Phys. **104**, 2482 (1996).

[67] This power series is only well founded for $\Delta\gamma_{||}^{ZPVA}$, but not for $\Delta\gamma_{K}^{ZPVA}$. We use it here nevertheless also for the Kerr hyperpolarizability, since the difference between $\gamma_{||}$ and γ_K is for N_2 in the considered frequency range small and we expand here only a small correction.

[68] Y. Luo, O. Vahtras, H. Ågren and P. Jørgensen, Chem. Phys. Lett. **205**, 555 (1993).

[69] D. P. Shelton, Mol. Phys. **60**, 65 (1987).

[70] D. P. Shelton, Phys. Rev. A. **36**, 3461 (1987).

[71] A. D. Buckingham, M. P. Bogaard, D. A. Dunmur, C. Hobbs and B. J. Orr, Trans. Faraday Soc. **66**, 1548 (1970).

[72] D. M. Bishop and S. P. A. Sauer, J. Chem. Phys. **108**, 8502 (1997).

[73] D. M. Bishop and J. Pipin, J. Chem. Phys. **103**, 4980 (1995).

[74] D. M. Bishop and B. Kirtman, J. Chem. Phys. **95**, 2646 (1991).

[75] A. D. Buckingham and B. J. Orr, Trans. Faraday Soc. **65**, 673 (1969).

[76] D. A. Dunmur, D. C. Hunt and N. E. Jessup, Mol. Phys. **37**, 713 (1979).

[77] D. P. Shelton, Phys. Rev. A. **34**, 304 (1986).

[78] J. M. Luis, J. Martí, M. Duran, J. L. Andr'es, B. Kirtman, J. Chem. Phys. **108**, 4123 (1998).

[79] C. Hättig, Mol. Phys. **94**, 455 (1998).

[80] C. Hättig, Chem. Phys. Lett. **296**, 245 (1998).

[81] A. D. Buckingham and H. C. Longuet-Higgins, Mol. Phys. **14**, 63 (1968).

[82] D. A. Imrie and R. E. Raab, Mol. Phys. **74**, 833 (1991).

[83] A. D. Buckingham and M. J. Jamieson, Mol. Phys. **22**, 117 (1971).

[84] S. Coriani, C. Hättig, P. Jørgensen, A. Rizzo and K. Ruud, J. Chem. Phys. **109**, 7176 (1998).

[85] C. Hättig and P. Jørgensen, Theor. Chim. Acc. **100**, 230 (1998).

[86] M. J. Jamieson, Chem. Phys. Lett. **176**, 467 (1991).

[87] M. J. Jamieson, Chem. Phys. Lett. **183**, 9 (1991).

[88] S. Coriani, C. Hättig and A. Rizzo, J. Chem. Phys. **111**, 7828 (1999).

[89] R. A. Kendall, T. H. Dunning and R. J. Harrison, J. Chem. Phys. **96**, 6796 (1992).

[90] D. E. Woon and T. H. Dunning, J. Chem. Phys. **100**, 2975 (1994).

[91] D. E. Woon and T. H. Dunning, J. Chem. Phys. **103**, 4572 (1995).

[92] H. Koch, A. S. de Merás, O. Christiansen and T. Helgaker, J. Chem. Phys. **104**, 4157 (1996).

[93] A. Kumar and W. J. Meath, Can. J. Chem. **63**, 1616 (1985).

[94] O. Christiansen, C. Hättig and J. Gauss, J. Chem. Phys. **109**, 4745 (1998).

[95] A. D. Buckingham, R. L. Disch and D. A. Dunmur, J. Am. Chem. Soc. **90**, 3104 (1968).

[96] G. A. Victor, A. Dalgarno and A. J. Taylor, J. Phys. B. **1**, 13 (1968).

[97] A. Dalgarno and A. E. Kingston, Proc. R. Soc. A. **259**, 424 (1960).